Cell

Substrate-Specific Translocational Attenuation during ER Stress Defines a Pre-Emptive Quality Control Pathway

Sang-Wook Kang,[1,4] Neena S. Rane,[1,4] Soo Jung Kim,[2] Jennifer L. Garrison,[3] Jack Taunton,[3] and Ramanujan S. Hegde[1,*]
[1] Cell Biology and Metabolism Branch, National Institute of Child Health and Human Development, National Institutes of Health, 18 Library Drive, Building 18T, Room 101, Bethesda, MD, 20892, USA
[2] Functional Genomic Research Center, Korea Research Institute of Bioscience and Biotechnology, Daejeon, 305-333, Korea
[3] Department of Cellular and Molecular Pharmacology, University of California, San Francisco, San Francisco, CA, 94107, USA
[4] These authors contributed equally to this work.
*Contact: hegder@mail.nih.gov
DOI 10.1016/j.cell.2006.10.032

SUMMARY

Eukaryotic proteins entering the secretory pathway are translocated into the ER by signal sequences that vary widely in primary structure. We now provide a functional rationale for this long-observed sequence diversity by demonstrating that differences among signals facilitate substrate-selective modulation of protein translocation. We find that during acute ER stress, translocation of secretory and membrane proteins is rapidly and transiently attenuated in a signal sequence-selective manner. Their cotranslational rerouting to the cytosol for degradation reduces the burden of misfolded substrates entering the ER and represents a pathway for pre-emptive quality control (pQC). Bypassing the pQC pathway for the prion protein increases its rate of aggregation in the ER lumen during prolonged stress and renders cells less capable of viable recovery. Conversely, pharmacologically augmenting pQC during ER stress proved protective. Thus, protein translocation is a physiologically regulated process that is utilized for pQC as part of the ER stress response.

INTRODUCTION

Eukaryotic proteins destined for the extracellular environment, cell surface, or compartments of the secretory pathway are first translocated across or integrated into the endoplasmic reticulum (ER) membrane (Wickner and Schekman, 2005). Their initial segregation to the ER requires a signal sequence, often encoded at the N terminus, that is cotranslationally recognized by the signal recognition particle (SRP) (Shan and Walter, 2005). The SRP-ribosome-nascent chain complex is subsequently targeted, via an interaction with the SRP receptor, to an ER protein translocon whose central channel is composed of the Sec61 complex (Osborne et al., 2005). The signal sequence is recognized again, this time by the Sec61 complex, to facilitate insertion of the nascent chain into the translocation channel and tight docking of the ribosome at the translocon (Jungnickel and Rapoport, 1995). Further protein synthesis is accompanied by Sec61-mediated translocation of the nascent chain across the ER membrane, or in the case of membrane proteins, integration into the lipid bilayer.

These basic steps of substrate recognition, targeting, engagement of the translocon, and translocation are thought to be universally applicable to essentially all secretory and membrane proteins. Whether any step in this process can be modulated under certain cellular conditions to selectively regulate protein translocation remains unknown. However, a strictly constitutive system of translocation would seem unlikely since essentially every other basic cellular process (from transcription to protein synthesis to degradation) is regulated for at least some substrates at one time or another. How then might protein translocation be regulated?

Given the essential role of the signal sequence in mediating both targeting and initiation of translocation, any regulatory process would presumably involve modulation of signal sequence function. Although such modulation has yet to be demonstrated, a growing number of studies are beginning to question the widely held view that signal sequences are functionally equivalent and largely interchangeable. For example, analyses of signal sequence-translocon interactions suggest an unexpectedly broad range of efficiencies in initiating translocation (Kim et al., 2002). Surprisingly, only a minority of signal sequences, such as the one from the well-studied model secretory hormone Prolactin (Prl), are highly efficient in vitro and in vivo (Kim et al., 2002; Levine et al., 2005). These same efficient

signal sequences also seem to be the only signals that do not depend substantially on accessory translocon components like TRAM (Voigt et al., 1996) and the TRAP complex (Fons et al., 2003) for translocation in vitro. If the only role for a signal sequence was to guarantee translocation across the ER, it is difficult to rationalize the existence of such diversity in sequence, efficiency, or complexity in their requirements for additional factors. Yet, these functional differences in efficiency are often evolutionarily conserved (Kim et al., 2001, 2002), even in instances in which inefficiencies in translocation would appear disadvantageous.

A particularly notable example is the signal sequence from the mammalian Prion protein (PrP), which is detectably less efficient in its interaction with the translocon than the signal from Prl (Rutkowski et al., 2001; Kim et al., 2002; Levine et al., 2005). In vivo, slight inefficiency of the PrP signal constantly generates a nontranslocated cytosolic form of PrP (cyPrP) that is degraded by the proteasome (Drisaldi et al., 2003; Rane et al., 2004). Although cyPrP represents a very low abundance form of PrP under normal conditions, it rapidly accumulates and aggregates upon inhibition of the proteasome (Ma and Lindquist, 2002; Drisaldi et al., 2003; Rane et al., 2004). CyPrP and the aggregates formed from it can be cytotoxic in cultured cells (Ma et al., 2002; Rane et al., 2004; Grenier et al., 2006) and cause neurodegeneration when generated in transgenic mice (Ma et al., 2002).

Similarly, slight inefficiency of the PrP signal sequence also permits the generation of ^{Ctm}PrP (Kim and Hegde, 2002), a transmembrane form of PrP whose slight overrepresentation can lead to neurodegeneration in mice and humans (Hegde et al., 1998a, 1999). Remarkably, the generation of both cyPrP and ^{Ctm}PrP can be markedly reduced or even eliminated simply by replacing the PrP signal sequence with the more efficient signal from Prl (Rutkowski et al., 2001; Kim et al., 2002; Rane et al., 2004). Even ^{Ctm}PrP-favoring mutations in the mature domain of PrP that ordinarily cause neurodegeneration can be reversed by increasing signal sequence efficiency (Kim and Hegde, 2002). Based on these findings, it is puzzling that the signal sequence of PrP has not evolved a few amino acid changes that increase its hydrophobicity to improve its functional efficiency. Yet, comparisons across multiple species have revealed that, although several polymorphic changes have occurred in the PrP signal (Schatzl et al., 1995), its slight but measurable inefficiency is precisely maintained for unknown reasons (Kim et al., 2001).

To resolve this apparent paradox, we hypothesized that differences between signal sequences among substrates might allow translocation to be modulated selectively under certain cellular conditions. Hence, there may exist situations when a seemingly imperfect signal sequence (such as from PrP), although potentially detrimental under some conditions, has additional (and beneficial) functionality that is not available with a ''constitutive'' and maximally efficient signal sequence (such as from Prl). In exploring this concept for PrP, we have now discovered a stress-induced pathway of translocational attenuation that acts to minimize PrP entry into and misfolding within the ER lumen. Remarkably, this pathway appears to be broadly utilized by the cell for many substrates in a signal sequence-dependent manner. Thus, the long-observed diversity in signal sequences (von Heijne, 1985) appears to encode regulatory information that permits the cell to selectively modulate translocation in a substrate-specific manner. These findings not only reveal protein translocation as a regulated rather than constitutive process but also identify a previously unappreciated protective response to ER stress.

RESULTS AND DISCUSSION

Reduced Translocation of PrP into the ER during ER Stress Defines a pQC Pathway

To look for potential examples of translocational regulation, we sought to identify conditions when the translocation of PrP is differentially modulated relative to Prl. A logical situation is during ER stress (Rutkowski and Kaufman, 2004), when entry into the ER of certain misfolding-prone proteins such as PrP may be disadvantageous to the cell. We therefore analyzed biosynthesis of PrP, Prl, and GFP (a cytosolic control) in pulse-labeled cultured cells acutely treated with two qualitatively different ER stressors: DTT, a reducing agent that induces ER stress by preventing productive folding of many secretory and membrane proteins, and thapsigargin (Tg), which depletes ER Ca^{2+} and influences chaperone function. Relative to untreated cells, Tg- and DTT-treated cells showed translational attenuation (see Figure S1 in the Supplemental Data available with this article online). This general translational inhibition was quantitatively mirrored by GFP and Prl (Figure 1A). Furthermore, all of the Prl synthesized under stressed and nonstressed conditions was processed by signal peptidase (Figure 1A; see also Figure 1D) and found by fractionation to be noncytosolic (data not shown). Although total PrP synthesis during Tg and DTT stress was attenuated to approximately the same levels as Prl and GFP, the amount of fully glycosylated PrP was preferentially reduced. The loss of glycosylated PrP was accompanied by a corresponding relative increase in the unglycosylated forms (asterisk, Figure 1A), at least some of which appeared to still contain an uncleaved signal sequence (S.-W.K. and R.S.H., unpublished data; Orsi et al., 2006; see Supplemental Data, Note 1).

Among the various possible reasons for this observation (see Supplemental Data, Note 2), the explanation proved to be a selective decrease in PrP translocation (but not Prl) during ER stress. This could be shown by domain swap experiments in which signal sequences were exchanged between PrP and Prl. Fusion of the Prl signal to PrP (Prl-PrP) now allowed Prl-PrP to be glycosylated with comparable efficiency in both untreated and DTT-stressed cells, with the decrease in fully glycosylated Prl-PrP during the stress paralleling the degree of

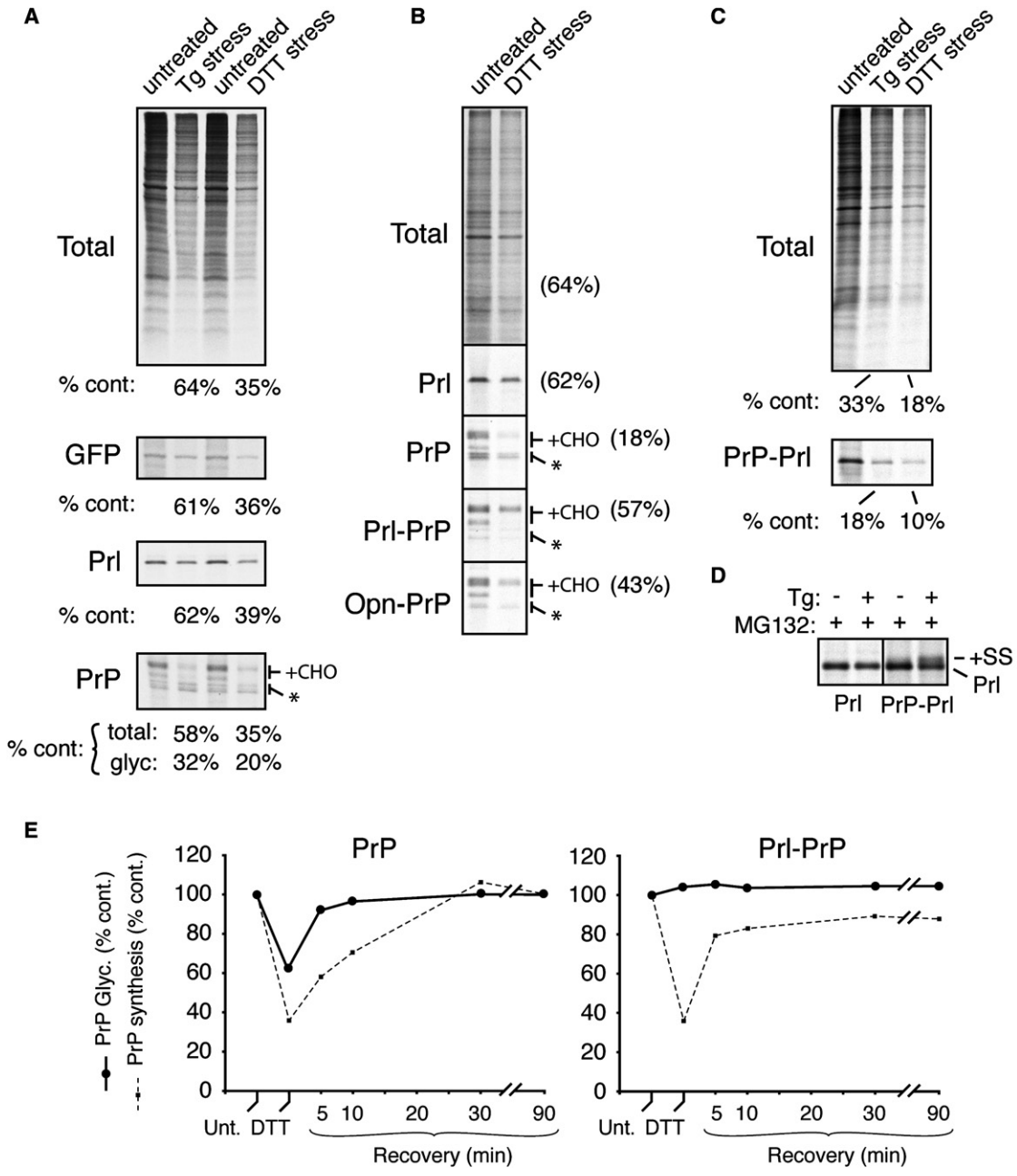

Figure 1. Signal Sequence-Specific Translocational Attenuation of PrP during Acute Stress

(A) Immunoprecipitation of transfected products (GFP, Prl, or PrP) from pulse-labeled (15 min) cultured HeLa cells treated for 30 min with 10 μM Tg or 10 mM DTT. Radiolabeled products recovered from stressed cells were quantified relative to untreated cells. For PrP, the amount of glycosylated species (+CHO) was also quantified separately. Asterisk is unglycosylated PrP.

(B) The indicated constructs were analyzed as in (A), except COS-7 cells were used, labeling was for 10 min, and 100 μM ALLN (a proteasome inhibitor) was included.

(C) PrP-Prl was analyzed and quantified as in (A).

(D) Prl and PrP-Prl were immunoprecipitated from pulse-labeled transfected cells treated with 10 μM Tg in the presence of 10 μM MG132 (a proteasome inhibitor) as indicated. Note that PrP-Prl (but not Prl) generates signal sequence-containing precursor (+SS, indicative of nontranslocated protein) in a stress-dependent manner, illustrating its translocational attenuation.

(E) Time course of recovery from translocational attenuation. COS-7 cells that were either untreated, acutely treated (30 min) with 10 mM DTT, or recovered for between 5 and 90 min were pulse labeled for 10 min and analyzed by immunoprecipitation of PrP. The efficiencies of glycosylation (solid line) and synthesis (dashed line) of either PrP (left graph) or Prl-PrP (right graph) relative to untreated cells are plotted.

translational attenuation (Figure 1B). A similar effect was also observed (albeit to a lesser extent) with another efficient signal sequence (from the protein Osteopontin [Opn]). Comparable results were also seen with Tg stress and validated further by cell fractionation experiments (Figure S3). Conversely, PrP-Prl biosynthesis was decreased below that attributable to general translational attenuation during acute ER stress (Figure 1C), with detection of a nontranslocated precursor when the proteasome is inhibited (Figure 1D).

Stress-dependent attenuation of PrP translocation was initiated almost immediately upon addition of the stressor (within ~5 min; data not shown). Furthermore, reversal of translocational attenutation occurred within minutes of removing the stress, even faster than recovery from translational attenuation (Figure 1E). Similar effects were observed in a variety of cell types (albeit to different extents) with both DTT and Tg (data not shown). Notably, other (non-ER) cellular stressors that also cause translational attenuation (such as serum starvation or amino acid deprivation) did not influence PrP translocation (data not shown). Based on these results, we conclude that *during* acute ER stress, a significant amount of nascent PrP is rerouted in a signal sequence-selective manner from its normal fate of being translocated into the ER to a pathway of proteasome-mediated degradation. We have termed this process "pre-emptive" quality control (pQC) to denote a pathway by which proteins are cotranslationally triaged for degradation at a step in their biosynthesis *before* they engage the conventional quality control systems in the ER lumen. The machinery utilized for degradation of translocationally aborted proteins during pQC remains to be identified but could potentially involve the recruitment of chaperones to the translocon by $p58^{IPK}$ (Oyadomari et al., 2006).

PrP Is Susceptible to Terminal Misfolding in the ER during Stress

Given that the functional properties of the PrP signal sequence appear to be evolutionarily conserved (Kim et al., 2001, 2002), we hypothesized that stress-dependent translocational attenuation of PrP may provide some benefit to the cell. One possibility is that translocational attenuation serves to avoid an adverse consequence of continued translocation during ongoing ER stress. Indeed, PrP translocated into the ER during DTT-induced stress was more prone to aggregation (as judged by decreased solubility in detergent solution) than newly synthesized PrP made in unstressed cells (Figure 2A). This effect was rapidly reversed (within minutes) upon removal of the stressor, at which point the PrP entering the ER lumen was again made in a soluble form. Pulse-chase experiments showed that PrP translocated into the ER during stress was prevented from subsequent exit to post-ER compartments (Figure S4A), further supporting the conclusion that it was misfolded.

Misfolded PrP in the ER was capable of being refolded and trafficked out of the ER, provided the stressor was removed promptly (within ~15 min; Figure 2B). However, continuing the stress an extra 30–360 min caused progressively larger proportions of the ER-lumenal PrP to become terminally misfolded, being retained in the ER in a largely insoluble state for prolonged times (Figures 2B and 2C and Figure S4B). Western blotting of total lysates from these same cells demonstrated that, after 6 hr of stress, the ER form of PrP had accumulated to ~30%–50% of total PrP (bottom panels, Figure 2C). This misfolded PrP persisted for the ensuing 20 hr despite ER function returning to normal (as judged by replenishment of fully mature PrP [the "post-ER" form] on the cell surface). Importantly, artificially retaining PrP in the ER lumen using brefeldin A (BFA) did not cause it to become insoluble (N.S.R. and R.S.H., unpublished data) or incapable of subsequent trafficking upon BFA removal (Figures S4C and S4D). Thus, the results in Figure 2 illustrate that PrP entering the ER during acute ER stress is prone to terminal misfolding and aggregation, after which it is neither refolded nor degraded efficiently, even if the stressor is subsequently alleviated. This terminal misfolding occurs over time scales of under an hour (e.g., Figure 2B and Figure S4B), well before the transcriptional responses to ER stress have had an opportunity to upregulate the ER biosynthetic and folding machinery (Yoshida et al., 2003).

The Consequences of Bypassing the pQC Pathway

The relative ease with which PrP becomes irrevocably misfolded in the ER lumen combined with its comparatively rapid degradation in the cytosolic environment suggest that stress-dependent translocational attenuation (i.e., access to the pQC pathway) may be a protective response to ER stress. To investigate this hypothesis, we determined the consequences of denying PrP access to the pQC pathway. We therefore generated stable cell lines that overexpress either PrP (which is subject to pQC) or Opn-PrP (which is largely refractory to pQC). The cell lines were analyzed by western blotting, immunofluorescence, and glycosidase digestion to confirm comparable expression, localization, and trafficking of PrP (Figures S5A–S5C).

When these same cells were subjected to DTT stress, Opn-PrP progressively accumulated the glycosylated ER form at a noticeably higher rate than PrP over the course of 8 hr (Figure 3A). Importantly, simply preventing ER-to-Golgi transport with BFA (which does not acutely induce ER stress and does not mediate translocational attenuation; data not shown) caused the accumulation of the ER form at comparable rates for both PrP and Opn-PrP (Figure S5D). Thus, the rate of entry into the ER is very similar for PrP and Opn-PrP in the absence of ER stress but differs sufficiently during stress to influence the accumulation of misfolded ER-lumenal PrP. Remarkably, the increased rate of misfolded ER-lumenal Opn-PrP accumulation led to a diminished capacity to recover from the ER stress, as measured using a cell replating viability assay (Figures 3B and 3E). Similar effects on viability were also seen with other ER stressors (Figure 3E). By contrast,

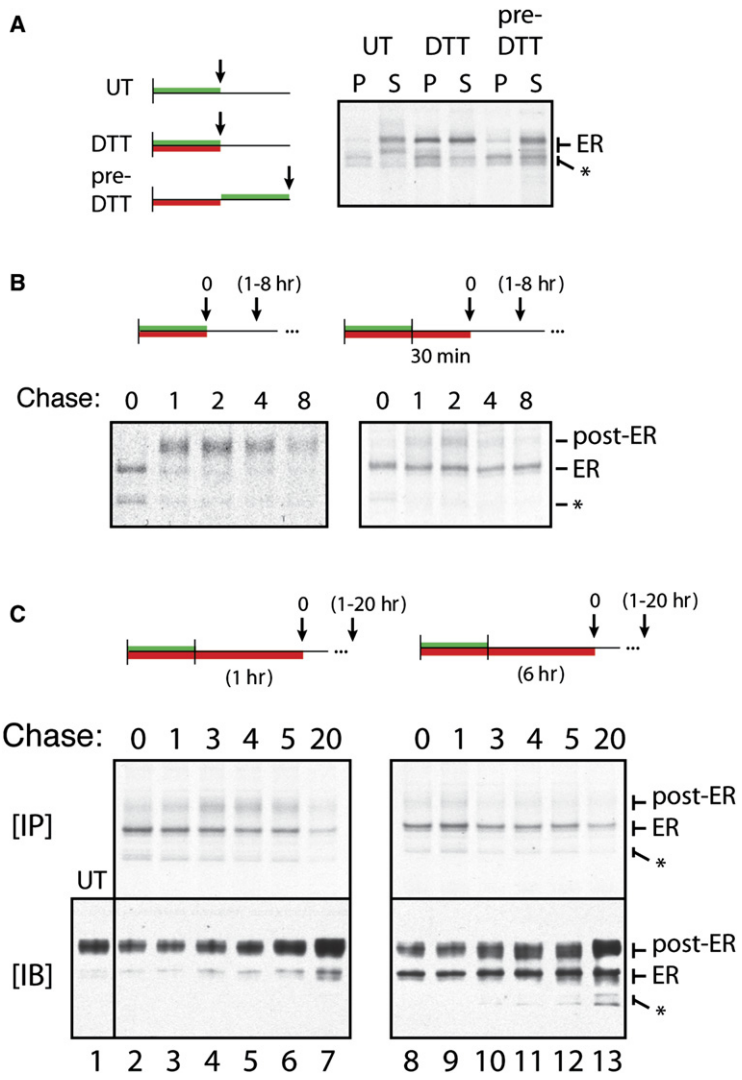

Figure 2. Terminal Misfolding of PrP during Prolonged ER Stress

(A) The left panel shows treatment protocols using N2a cells for 30 min pulse labeling (green bars) and 30 min treatment with 10 mM DTT (red bars) relative to harvesting (arrows) and analysis by solubility assays. PrP in the detergent-insoluble (P) and -soluble (S) fractions was recovered by immunoprecipitation and visualized by autoradiography. The core-glycosylated ER form and nonglycosylated species (*) of PrP are indicated.

(B) Treatment protocols for labeling, DTT treatment, and chase (for 1–8 hr) prior to harvesting and immunoprecipitation are shown above the respective autoradiographs. Unglycosylated (*), core-glycosylated (ER), and complex glycosylated (post-ER) forms of PrP are indicated.

(C) Cell lysates from the indicated treatment protocols were divided and analyzed for radiolabeled PrP by immunoprecipitation and autoradiography ([IP], top panels) or for total PrP by immunoblots ([IB], bottom panels).

partial inhibition of the proteasome in these same cells caused a nonglycosylated form of PrP (but not Opn-PrP) to accumulate in the cytosol (Figure 3C). Replating viability assays showed the PrP cells to be less viable than Opn-PrP cells after chronic proteasome inhibition (Figures 3D and 3E).

We conclude from Figure 3 that inefficiencies in PrP translocation necessitate constant proteasomal degradation of nontranslocated material that can be highly aggregation prone and cytotoxic if left undegraded. Although the more-efficient Opn signal sequence minimizes these problems, it becomes a liability when the ER environment is compromised. Under these conditions, constitutively high translocation efficiency of Opn-PrP results in a higher rate of accumulation of misfolded PrP in the ER lumen and decreased recovery from the stressor when compared to PrP. Thus, bypassing stress-mediated translocational attenuation of PrP sensitizes cells to ER stress. This result suggests that, for PrP, the pQC pathway is a physiologically important facet of the cellular response to an altered folding environment in the ER. The basis of this effect correlated directly with the minimization of protein misfolding, aggregation, and accumulation in the ER lumen.

Accentuating the pQC Pathway during ER Stress Is Protective

The increased sensitivity of Opn-PrP-expressing cells to ER stress suggests that constitutive translocation under these conditions is more detrimental than rerouting PrP directly to the cytosol. Although a reduction in PrP translocation might have seemed problematic given previous results identifying cytosolic PrP as highly cytotoxic (Ma et al., 2002) and aggregation prone (Ma and Lindquist, 2002; Drisaldi et al., 2003; Rane et al., 2004; Grenier et al., 2006), this proved not to be the case. Pharmacologic inhibition of PrP translocation in vivo with cotransin (CT; see Figures S3B and S5E) for up to 24 hr did not lead to the accumulation of PrP aggregates in the cytosol

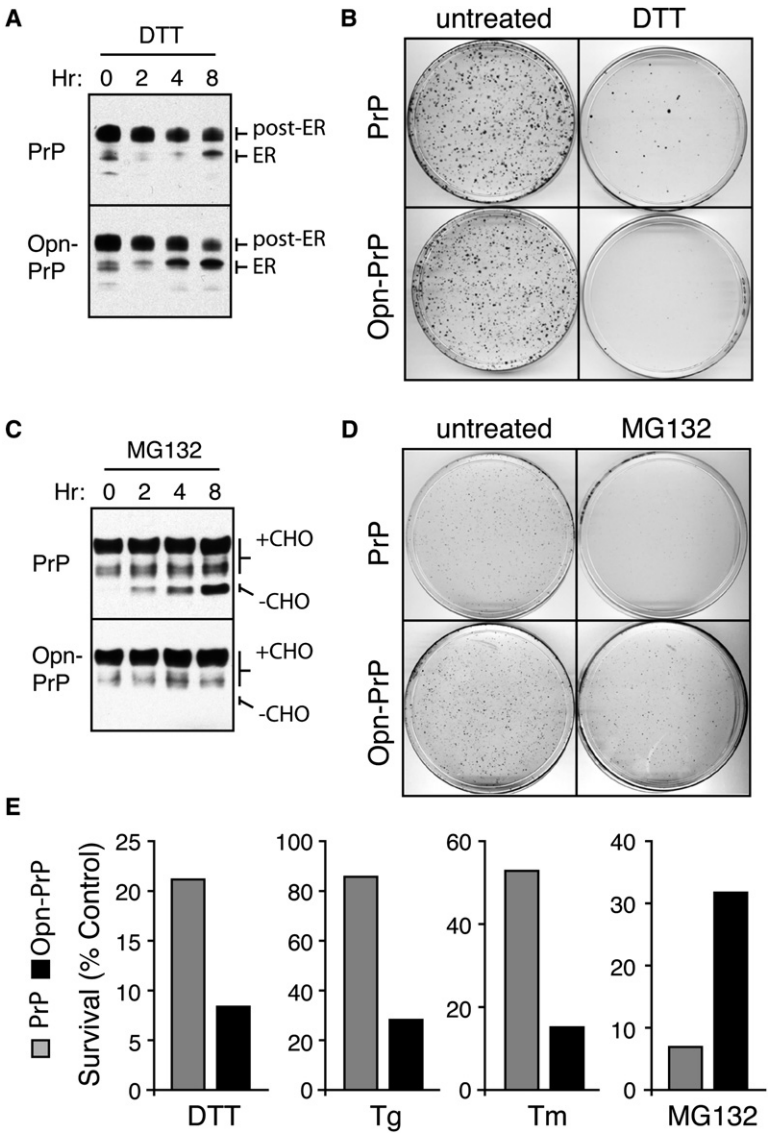

Figure 3. Consequences of Bypassing the pQC Pathway for PrP

(A) N2a cells stably expressing PrP or Opn-PrP were treated for 0–8 hr with 10 mM DTT and analyzed for total PrP by immunoblot. Note the increased accumulation of the ER form in Opn-PrP cells relative to PrP cells, especially obvious at the 4 hr time point.

(B) Cells stably expressing PrP or Opn-PrP were treated with 10 mM DTT for 24 hr, replated in normal media, and visualized 10 days later by staining with crystal violet.

(C) Cells stably expressing PrP or Opn-PrP were treated for 0–8 hr with 5 μM MG132 and analyzed for total PrP by immunoblot. Note the increased accumulation of unglycosylated species (−CHO) for PrP, but not for Opn-PrP.

(D) Cells treated with 5 μM MG132 for 24 hr were replated in normal media and visualized 8 days later by staining with crystal violet.

(E) Quantification of replating viability assays for survival of cells expressing PrP (gray bars) or Opn-PrP (black bars) after the indicated treatments for 24 hr (5 μM MG132), 6 hr (10 mM DTT), 18 hr (1 μg/ml Tunicamycin; Tm) or 5 min (5 μM Tg).

or obvious cell death (Figures 4A and 4D). Instead, total PrP simply decreased over time due to turnover of preexisting PrP from the cell surface and rapid degradation of nontranslocated PrP (which could be visualized by proteasome inhibition; Figure 4A).

Upon removal of CT, cell surface PrP was readily replenished, with no accumulation of cytosolic PrP even over the course of 72 hr (Figures 4B and 4C). This contrasted sharply with proteasome inhibition, where aggregates of nontranslocated PrP appeared within a few hours (Figure 3C) and persisted long after alleviation of proteasome inhibition (Figure 4C). Furthermore, once initiated, PrP aggregates continue to accumulate (by a poorly understood "self-propagation" process that amplifies even trace amounts of PrP aggregates; Ma and Lindquist, 2002), eventually leading to decreased cell viability (Figure 3D). The consequences of proteasome inhibition on PrP accumulation and cell viability were worsened by simultaneous inhibition with CT (Figure 4D) or DTT (Figure S6A), both of which result in increased delivery of PrP to the cytosol.

Since even a complete block in PrP translocation is not inherently cytotoxic, we could ask whether accentuating translocational attenuation of PrP could be protective from the consequences of prolonged ER stress. Indeed, simultaneous treatment with CT during chronic DTT stress was able to partially improve viability for PrP-expressing cells (Figure 4E). This effect was due at least in part to the effect of CT on PrP, since a similar rescue was not effected for cells expressing Opn-PrP (Figure 4E), whose translocation is only partially inhibited by CT (Figure 4A and Figure S5E). With less-severe DTT stress, even Opn-PrP cells or nontransfected cells could be rescued by simultaneous treatment with CT (Figure S6B and data not shown), presumably because CT inhibits several other signal-containing proteins to reduce the overall burden of substrates entering the ER (see Figure S7). Thus,

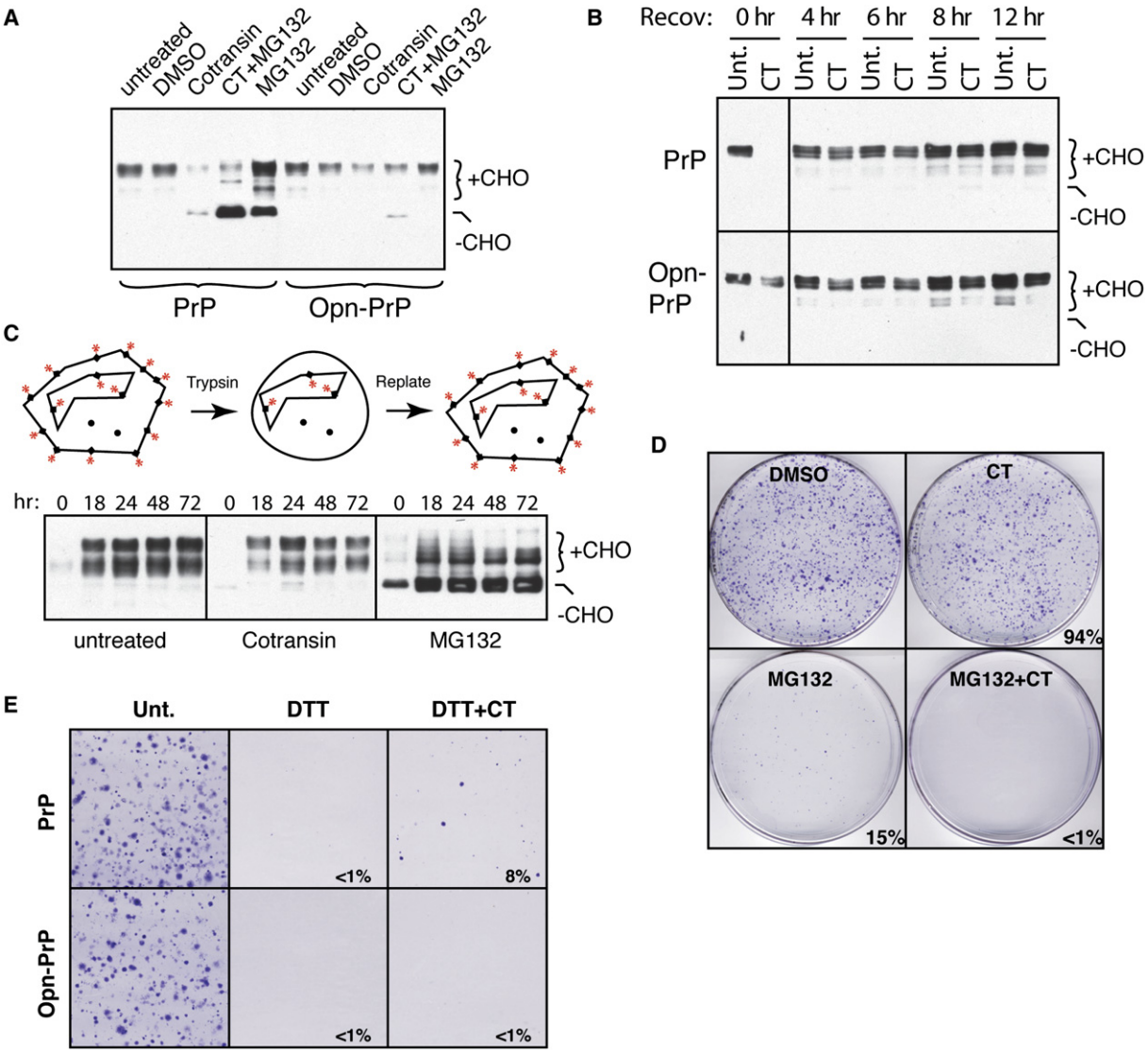

Figure 4. Pharmacologic Induction of pQC during Prolonged ER Stress Is Protective

(A) PrP and Opn-PrP cells were treated for 6 hr (5 μM CT, 5 μM MG132, and/or 0.1% DMSO) and analyzed by immunoblotting. The glycosylated (+CHO) and unglycosylated (−CHO) forms of PrP are indicated.

(B) PrP and Opn-PrP cells treated for 12 hr with solvent (0.1% DMSO) or 5 μM CT were recovered in regular media for the indicated times and analyzed by immunoblotting for PrP.

(C) PrP-expressing cells were treated for 4 hr with either 5 μM CT or 5 μM MG132, followed by trypsinization and replating in normal media for the indicated times before harvesting and analysis by immunoblotting. Diagram illustrating the experimental design is shown.

(D) PrP-expressing cells treated for 12 hr as indicated were replated in normal media and visualized 10 days later by staining with crystal violet. Quantification of viability relative to control is indicated.

(E) PrP and Opn-PrP cells treated for 24 hr as indicated were replated in normal media and visualized 10 days later by staining with crystal violet. Quantification of viability relative to control is indicated.

complementary to the adverse consequences of bypassing pQC (Figure 3), accentuating pQC for PrP is protective during ER stress.

The pQC Pathway Is Broadly Utilized

Since highly efficient signals like those from Prl and Opn are found on a relative minority of proteins, we surmised that the pQC pathway might be utilized by many proteins in addition to PrP. To examine this idea, we took two parallel approaches: analysis of global translocation efficiency using N-linked glycosylation as a surrogate marker for entry into the ER, and individual analyses of various secretory and membrane proteins.

In the first approach (Figure 5A), pulse-labeled adherent cultured cells are first permeabilized with low concentrations of digitonin to selectively extract the cytosolic

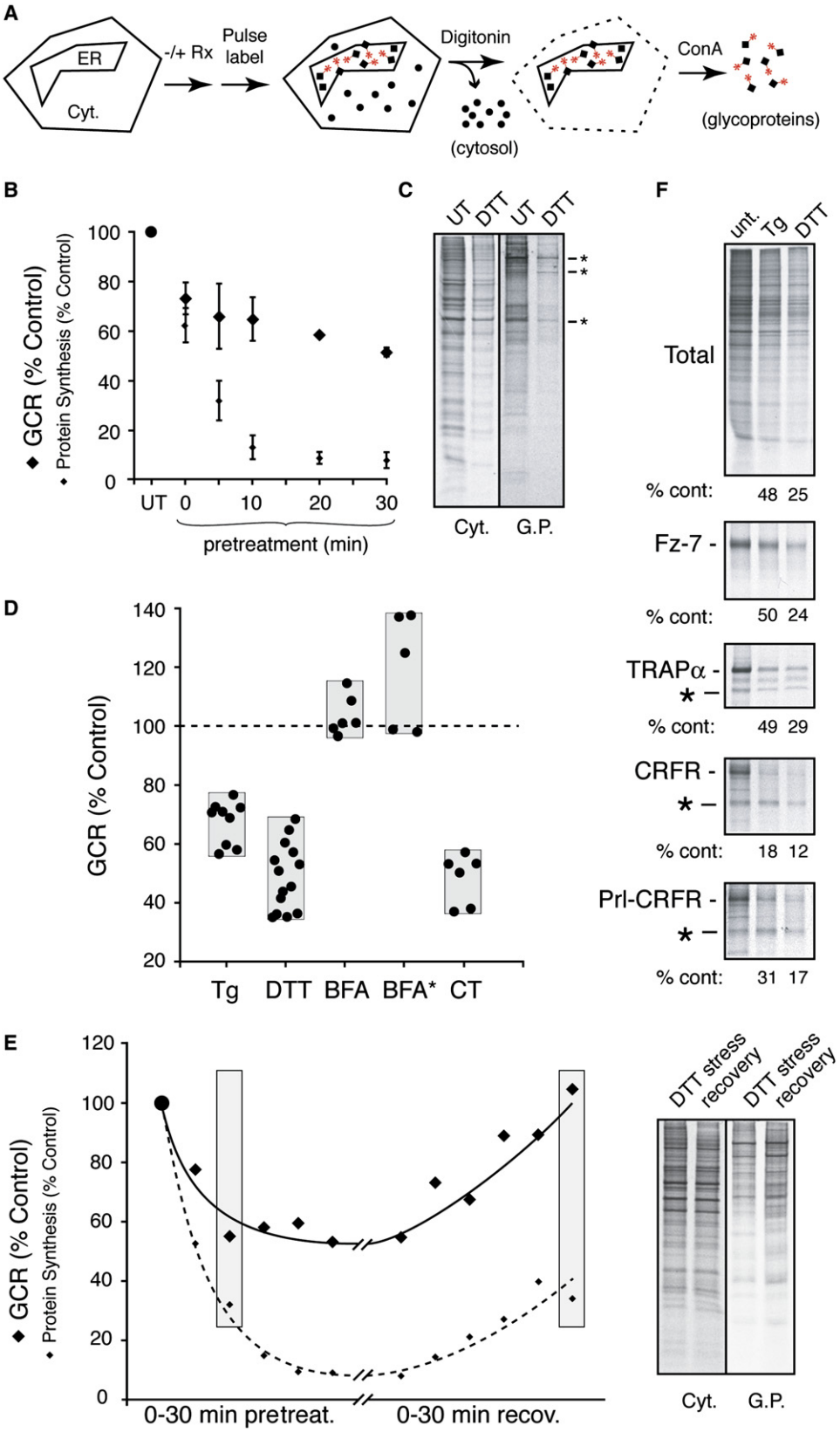
A
ER
Cyt.
-/+ Rx
Pulse label
Digitonin
(cytosol)
ConA
(glycoproteins)
B
GCR (% Control)
Protein Synthesis (% Control)
100
80
60
40
20
0
UT 0 10 20 30
pretreatment (min)
C
UT DTT UT DTT
Cyt. G.P.
F
unt. Tg DTT
Total
% cont: 48 25
Fz-7 -
% cont: 50 24
TRAPα -
% cont: 49 29
CRFR -
% cont: 18 12
Prl-CRFR -
% cont: 31 17
D
GCR (% Control)
140
120
100
80
60
40
20
Tg DTT BFA BFA* CT
E
GCR (% Control)
Protein Synthesis (% Control)
120
100
80
60
40
20
0
0-30 min pretreat.
0-30 min recov.
DTT stress recovery
DTT stress recovery
Cyt. G.P.

contents. The remainder of the cell is then solubilized and the glycoproteins isolated by binding to immobilized concanavalin A (ConA). Quantitative analysis of the ConA and digitonin fractions by SDS-PAGE and phosphorimaging is used to derive a "glycoprotein-to-cytosolic protein ratio" (GCR), a parameter that should change with any acute changes to the efficiency of protein sequestration into the ER. This approach was tested and validated using CT to directly influence translocation efficiencies (Figure S7).

Upon acute DTT stress, the GCR promptly decreased by ~30% within 10 min (Figure 5B). At very short times after DTT treatment, several glycoproteins (but no cytosolic proteins) were selectively reduced to a much greater level than others (Figure S8). At longer treatment times (Figure 5C), there was both a greater degree of translational attenuation and a larger number of glycoproteins whose levels were yet lower (Supplemental Data, Note 3). Interestingly, some glycoproteins were far less affected than others at all treatment times (asterisks in Figure 5C).

Compilation of numerous experiments examining GCR upon treatment of cells with various agents (Figure 5D) revealed a similar, albeit smaller, effect with the ER stressor Tg. Time course experiments with Tg also showed a rapid onset of decreased GCR, concomitant with or slightly faster than translational attenuation (data not shown). Treatments with BFA, serum starvation, or amino acid starvation did not show obvious changes in GCR (Figure 5D and data not shown). The stress-mediated reduction in GCR was rapidly reversible within minutes after removal of the stressor (Figure 5E), well before translational attenuation was reversed. This argued that the GCR effect was not a direct consequence of decreased translation per se. For example, direct comparison of two samples with essentially equal translational repression (~70%) but markedly different GCR clearly illustrated the selective effect on glycoproteins relative to cytosolic proteins (Figure 5E).

The rapid, reversible, and substrate-selective reduction of glycoprotein biosynthesis (beyond that accounted by translational attenuation alone) was reminiscent of stress-mediated signal sequence-specific translocational attenuation of PrP, suggesting that changes in GCR could potentially be caused by changes in protein translocation efficiencies. The rapid induction (less than 10 min) argued against a transcriptional suppression of glycoproteins, while the rapid reversibility was not compatible with a major contribution from selective degradation of transcripts coding for glycoproteins (Hollien and Weissman, 2006). Furthermore, pulse-chase and inhibitor experiments (Figure S9) argued against a substantial increase in the retrotranslocation (or ERAD) pathway at such short times after initiating stress. Together, these findings pointed toward translocational attenuation as the principal basis for the decreased GCR observed during acute ER stress.

To verify this conclusion further, we examined several individual proteins. Among our still-cursory survey, we found that some membrane glycoproteins such as TRAPα, Frizzled-7, vesicular stomatitis virus glycoprotein (VSVG), and vascular cell adhesion molecule (VCAM) were essentially unaffected in their biosynthesis during stress beyond that caused by translational attenuation (Figure 5F; S.-W.K. and R.S.H., unpublished data). By contrast, angiotensinogen, interferon-γ, and the corticotropin-releasing factor receptor (CRFR) were each attenuated to varying degrees during stress (Figure 5F; S.-W.K. and R.S.H., unpublished data). Replacement of the CRFR signal sequence with that from Prl partially rescued its stress-dependent attenuation (Figure 5F), further validating the fact that the effect on CRFR was at the level of its translocation into the ER. Thus, the pQC pathway is not unique to PrP and appears to be more broadly utilized based on both the glycoprotein profiling experiments and survey of several secretory and membrane proteins.

Reconstitution of Signal Sequence-Specific Translocational Attenuation In Vitro

To gain insight into the mechanisms underlying pQC, we sought to reconstitute its salient features in vitro. In initial experiments, we analyzed translocation of endogenous mRNAs using semipermeabilized cells pretreated with ER stressors (Supplemental Data, Note 4 and Figure S10). These experiments not only supported the conclusions from the in vivo studies but suggested that translocation is likely to be attenuated at the ER after nascent polypeptides are targeted to and docked at the translocon.

Figure 5. Analysis of Global Glycoprotein Biosynthesis during Acute ER Stress

(A) Experimental design.

(B) HeLa cells treated with 10 mM DTT for the indicated times were pulse labeled (for 15 min), fractionated, and quantified to determine the glycoprotein-to-cytosolic protein ratio (GCR). The GCR at each time point (normalized to untreated cells) is plotted along with the overall level of protein synthesis (mean ± SD for three experiments).

(C) Radiolabeled cytosolic proteins and glycoproteins from untreated and DTT-stressed (30 min) HeLa cells. Asterisks indicate bands that are minimally attenuated relative to other glycoproteins.

(D) GCR (normalized to untreated cells analyzed in parallel) for HeLa cells acutely treated (for 30 min) with 10 μM Tg, 10 mM DTT, 10 μg/ml BFA, or 10 μM CT. Each point represents an individual experiment, with the gray bar showing the range observed. BFA* indicates treatment for 12 hr.

(E) GCR (solid line) and overall translation (dotted line) was measured in cells pretreated for between 0 and 30 min with 10 mM DTT, or treated for 30 min followed by recovery in normal media for 0–30 min. Samples from time points shaded in gray are shown to the right. Note that *during* acute stress, many (but not all) glycoproteins are attenuated in their biosynthesis relative to the situation during recovery.

(F) Analysis as in Figure 1A of Frizzled-7 (Fz7), TRAPα, CRF1 receptor (CRFR), and Prl-CRFR by pulse labeling and immunoprecipitation from transiently transfected cells treated for 30 min with 10 μM Tg or 10 mM DTT. Asterisks indicate nonglycosylated forms of each glycoprotein (except Frizzled-7, in which a nonglycosylated form was not detectable). The amount of the translocated and glycosylated form generated under each condition is quantified relative to untreated cells. The decrease in Frizzled-7 and TRAPα paralleled the level of translational attenuation caused by the stress.

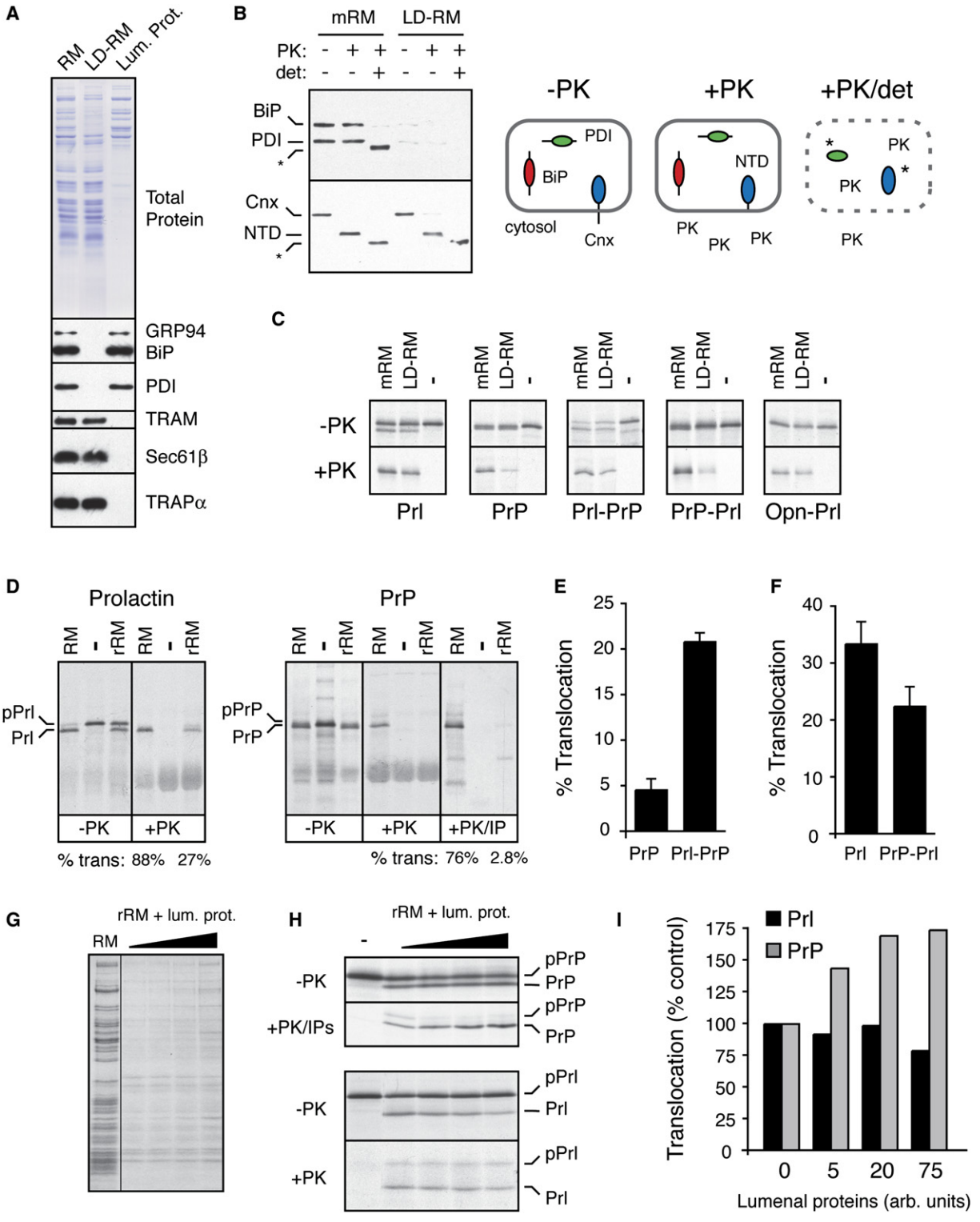

Figure 6. Reconstitution of Signal Sequence-Specific Translocational Attenuation In Vitro

(A) Selective removal of lumenal proteins from rough microsomes (RM) by treatment with 0.075% deoxyBigCHAP. Equivalent aliquots of RM, the lumenal protein-depleted RM (LD-RM), and lumenal protein fraction were analyzed by Comassie staining (top) and immunoblots for various lumenal and membrane proteins (bottom). Although not seen in this blot, semiquantitative blotting showed ~80%–90% depletion of BiP and PDI (data not shown).

One of the earliest events in the ER-stress response is thought to be the titration of lumenal chaperones by their association with an increased burden of misfolded proteins (Rutkowski and Kaufman, 2004). To determine whether this acute decrease in functionally available lumenal chaperones might directly influence translocation, we analyzed the in vitro translocation of Prl and PrP in rough microsomes (RM) containing or lacking lumenal contents. Soluble lumenal proteins were selectively extracted from RM with low concentrations of detergent well below those needed to solubilize membrane proteins. The resulting membranes (LD-RM) were substantially depleted (by ~80%–90%) of several lumenal chaperones (and, presumably, nonchaperone proteins) relative to mock-extracted RM (mRM), and both preparations were intact and of the correct orientation (Figures 6A and 6B).

While translocation of Prl was modestly decreased (by ~30%) in LD-RM, translocation of PrP was reduced by ~70% (Figure 6C). This decrease was largely reversed upon replacing the PrP signal sequence with that from Prl. Conversely, Prl translocation became more dependent on lumenal proteins when its signal sequence was replaced with that from PrP, but not from Opn. When lumenal proteins were depleted even more thoroughly (>98%) by reconstituting total detergent-solubilized membrane proteins into proteoliposomes (to generate rRM), the differential in translocation efficiencies between Prl and PrP widened: while both were translocated into RM with comparable efficiency (~75%–85%), translocation of PrP into rRM was nearly 10-fold lower than translocation of Prl (Figure 6D).

Translocation into rRM of Prl-PrP was several-fold more efficient that PrP (Figure 6E), while PrP-Prl translocation was modestly less efficient than Prl (Figure 6F). This result, along with the similar observations in LD-RM (Figure 6C), illustrates that the signal sequence contributes significantly to substrate-specific differences in the dependence on lumenal proteins for translocation. And finally, although coreconstitution of lumenal proteins into rRM was rather inefficient (Figure 6G; see Supplemental Data, Note 5), we could nonetheless detect a modest stimulatory effect on PrP translocation, but not Prl translocation (Figures 6H and 6I). Considered together, these in vitro analyses demonstrate that while translocation of PrP and Prl are comparably efficient under normal conditions, modulation of lumenal protein availability has a significantly greater impact on PrP translocation in a signal sequence-selective manner. These findings suggested that changes in the function and/or availability of lumenal proteins (such as chaperones) during acute ER stress in vivo could explain the substrate-specific effects on translocation.

Induction of pQC Correlates with Reduced Lumenal Chaperone Availability

To examine this idea, we assessed the biochemical state of lumenal chaperones in unstressed and acutely stressed cells. Because interactions between BiP and its substrates could be readily stabilized after cell lysis (by ATP depletion), we focused on this lumenal chaperone. During acute DTT stress, the amount of BiP that is unoccupied with substrate (as judged by its solubility and native size on sucrose gradients) decreased noticeably (Figure 7A). The remainder of BiP was engaged in heterogeneous complexes and recovered in a combination of the "insoluble" fraction, high-molecular-weight fractions of the sucrose gradient, and SDS-resistant material at the top of the gel (Figure 7B). Monitoring BiP levels in the insoluble fraction revealed a rapid reversal of this effect upon removal of the stressor (Figure 7C) that paralleled the time course of recovery from translocational attenuation (Figures 1E and 5E). The amount of unengaged PDI was also reduced (but much more modestly), while calnexin (Cnx) and calreticulin (Crt) were unchanged by this assay.

Although total chaperone levels were unchanged during the acute stress treatments employed in this study, recovery for ~16–20 hr led to substantial upregulation of BiP (and to a lesser extent PDI) due to induction of the unfolded protein response (Figure 7D). Even in this preconditioned state, treatment with acute ER stress led to decreased BiP levels in the soluble fraction (with corresponding increases in the insoluble fraction; Figure 7E and data not shown). However, the increased reservoir of BiP in

(B) Analysis of LD-RM and mock-extracted RM (mRM) for vesicle integrity and orientation by a protease protection assay. LD-RM and mRM were digested with Proteinase K (PK) in the absence or presence of detergent (det; 0.5% Triton X-100) and analyzed by immunoblotting for the N terminus of calnexin (Cnx), BiP, and PDI. The N-terminal lumenal domain of Cnx is indicated by NTD. Asterisks indicate core domains of Cnx and PDI that are resistant to complete protease digestion. A schematic of the results is shown.

(C) Analysis of protein translocation into mRM and LD-RM. The indicated constructs were translated in vitro without (–) or with membranes (either mRM or LD-RM) and analyzed for translocation by protease protection. Aliquots of the samples before and after PK digestion are shown. The relative translocation efficiency in LD-RM (relative to translocation in mRM) is indicated for each construct. All translation reactions contained a peptide inhibitor of glycosyation to simplify the analysis.

(D) Analysis of protein translocation in RM and rRM (proteoliposomes reconstituted from a total membrane protein extract of RM) as in (C). An aliquot of the PrP samples was also immunoprecipitated with anti-PrP (+PK/IP) to better visualize the translocation products. Translocation efficiencies are given below the lanes. The positions of precursor and processed products for Prl and PrP are indicated.

(E and F) The relative translocation efficiencies of the indicated constructs were analyzed in rRM and quantified from five experiments (mean ± SD). All constructs were translocated into RM with greater than 75% efficiency (data not shown).

(G) Coomassie stain of rRM reconstituted in the presence of increasing concentrations of lumenal proteins. Note that the concentration of lumenal proteins incorporated into the rRM is low and does not approach that found in RM (Supplemental Data, Note 5).

(H) Translocation of PrP and Prl was analyzed as in (D) using rRM containing increasing amounts of lumenal proteins. Note that in rRM, signal sequence cleavage is not complete, resulting in some translocation (and hence protease protection) of unprocessed protein.

(I) The experiment in (H) was quantified, normalized to translocation in rRM (lacking lumenal proteins), and graphed.

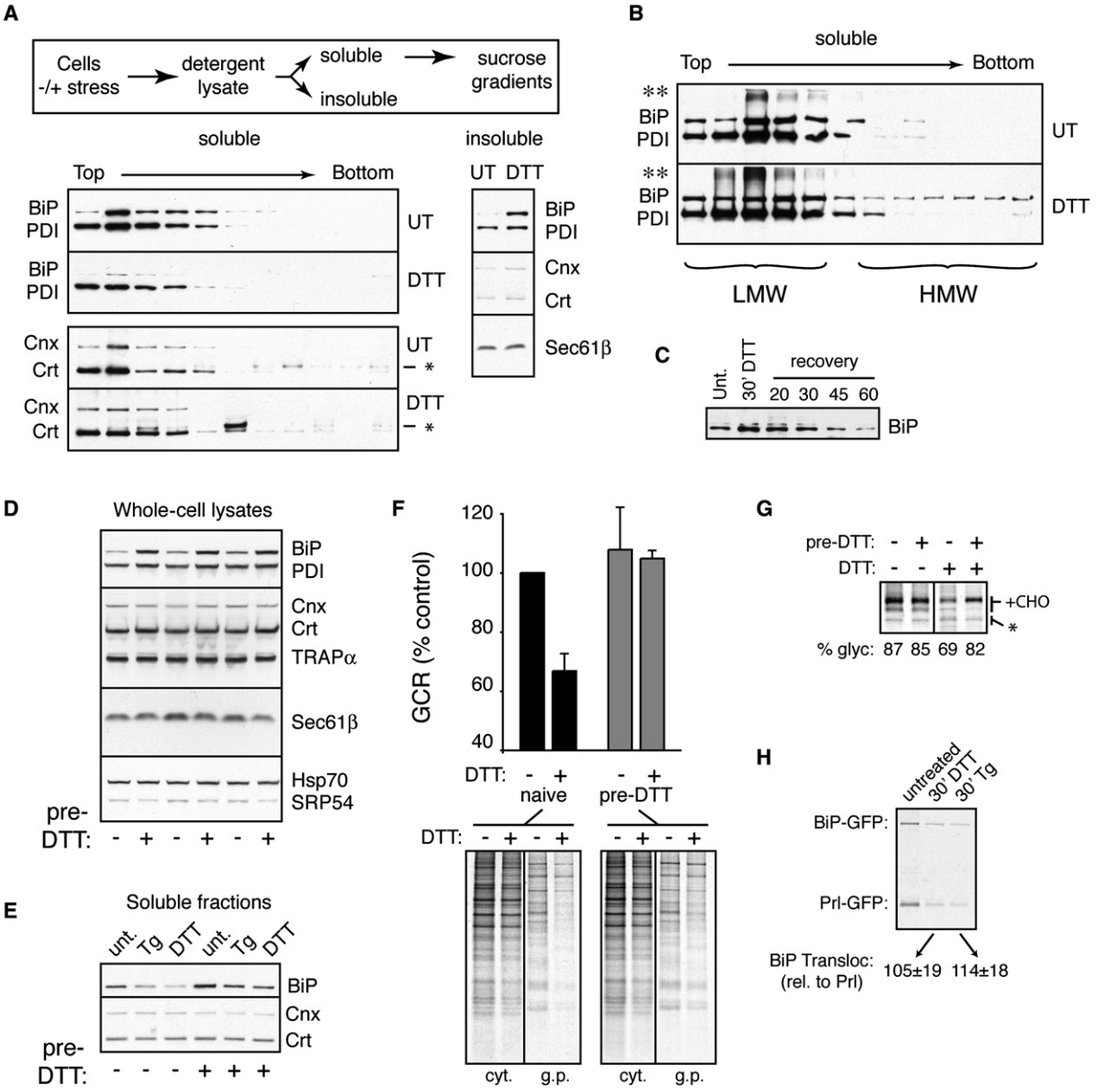

Figure 7. Changes in Lumenal Chaperone Availability Accompany pQC

(A) The sizes of chaperone-containing complexes were analyzed in unstressed or acutely stressed (10 mM DTT for 30 min) HeLa cells by detergent extraction, fractionation by sucrose gradients, and immunoblotting (outlined on top). Note the decrease in BiP (and to a lesser extent, PDI) in the soluble fractions, with a corresponding increase in the insoluble fraction. The band slightly larger than Crt (*) is a background band that was inconsistently observed in some lanes.

(B) Analysis of overloaded samples prepared as in (A) reveals increased amounts of BiP in both high-molecular-weight fractions (HMW) and previously described SDS-resistant complexes (**; see Marciniak et al. [2004]) in stressed cells relative to control cells.

(C) The level of BiP in the insoluble fraction of HeLa cells acutely treated with 10 mM DTT for 30 min or treated and recovered for between 20 and 60 min.

(D) The levels of various proteins were analyzed by immunoblotting in HeLa cells pretreated with 10 mM DTT for 1 hr followed by recovery for 18 hr. Triplicate samples are shown. Note induction of BiP and, to a lesser extent, PDI by the pretreatment protocol.

(E) Cells were either left untreated or preconditioned with DTT as in (D). Subsequently, the levels of BiP, Cnx, and Crt in the soluble fractions (prepared as in [A]) were analyzed by immunoblotting before or after acute stress for 30 min with 10 μM Tg or 10 mM DTT.

(F) Naive or DTT-preconditioned cells were analyzed for changes in GCR (mean ± SD for three replicates) upon acute ER stress for 15 min with 10 mM DTT. The autoradiograph from a representative experiment is shown.

(G) Naive or DTT-preconditioned cells were analyzed for changes in PrP translocation upon acute ER stress for 30 min with 10 mM DTT. Note that while naive cells showed translocational attenuation (as judged by decreased PrP glycosylation), preconditioned cells were largely refractory. Translational attenuation upon DTT stress was equal in both cells (data not shown).

preconditioned cells still left enough in the soluble fraction even during stress to maintain levels comparable to unstressed nonpreconditioned cells (compare lane 1 to lanes 5 and 6 in Figure 7E). Remarkably, preconditioned cells showed little or no translocational attenuation during acute stress, as judged by analyses of either the GCR (Figure 7F) or PrP biosynthesis (Figure 7G). Thus, using BiP as a marker, we find that the available (i.e., unengaged) levels of this lumenal chaperone correlate inversely with substrate-specific translocational attenuation. Interestingly, translocation of BiP, whose upregulation is a critical facet of the stress response, is not attenuated even during maximal acute stress (Figure 7H). Together with the biochemical analysis of translocation in vitro (Figure 6), these results point to rapid changes in lumenal chaperone availability and/or function during acute stress as one (but perhaps not the only) basis for substrate-specific translocational attenuation and pQC (see Supplemental Data, Note 6 for possible models).

Conclusions

This study illustrates that protein translocation into the ER lumen is not a constitutive or deterministic process but instead can be regulated in response to changes in cellular conditions. In the context of acute ER stress, changes in translocation efficiency are substrate specific, reversible, and physiologically important (see Supplemental Data, Note 7 and model in Figure S11). Selectivity of translocational attenuation is determined (at least in part) by signal sequences, whose length, hydrophobicity, charge, and amino acid composition vary widely between substrates (von Heijne, 1985). Our discovery that this structural diversity among signals imparts differential functionality during translocation provides a rationale for why signal sequences are often conserved in a substrate-specific manner (Kim et al., 2001; Kim et al., 2002) and appear to evolve more slowly than expected for such a highly variable motif (Williams et al., 2000).

In the case of PrP, a relative weak and modulatable signal sequence may be especially important for minimizing the risk of permanantly producing potentially toxic species in enclosed compartments like the ER lumen. A similar logic may apply to other misfolding-prone secretory and membrane proteins. An analogous (and non-mutually exclusive) explanation for signal sequence diversity is that certain highly overproduced secretory proteins like prolactin may need to contain signal sequences that can escape normal stress-induced attenuation mechanisms that might be induced during rapid changes in secretory activity. This rationale presumably applies to BiP, which sometimes needs to be translocated effectively even at high expression levels during ongoing ER stress. Thus, sequence differences among signal sequences may provide a means to regulate the translocation efficiency of some substrates independently of others for various physiological purposes.

Of note, the most efficient signal sequences (as judged in vitro) may prove to be the least regulatable. This is analogous to many other biological systems, in which optimal efficiency comes at a cost of reduced dynamic range. For example, highly regulatable promoters often have very low basal activity and are dependent on many accessory transcription factors, while extremely strong promoters are less modulatable. A similar concept may apply to translocation, in which signal sequences whose interactions with the translocon are highly efficient and less dependent on accessory factors are less amenable to modulation in *trans*. Such a view would provide a logical explanation for the otherwise paradoxical observation that most signal sequences appear to be less than maximally efficient (Kim et al., 2002; Levine et al., 2005).

The mechanism by which differences among signal sequences permit substrate-specific and stress-dependent attenuation of translocation remains to be studied. Intrestingly, the posttargeting interaction between the signal sequence and translocon (Jungnickel and Rapoport, 1995; Plath et al., 1998; Mothes et al., 1998) is not only highly variable (Kim et al., 2002) but is differentially influenced by *trans*-acting factors (Voigt et al., 1996; Fons et al., 2003) and small molecules (Garrison et al., 2005; Besemer et al., 2005). It is therefore tempting to speculate that such differences in the signal-translocon interaction are analogously exploited during ER stress for selective lumenal protein-dependent translocational attenuation to initiate pQC. Analysis of this step in mechanistic detail for multiple signal sequences that are either sensitive or refractory to translocational attenuation will be required to elucidate the molecular basis of substrate-specific regulation of translocation. The reconstitution of signal sequence-selective translocational attenuation in a biochemical system amenable to fractionation (Figure 6) should now facilitate these future studies.

EXPERIMENTAL PROCEDURES

Experiments in this study generally utilized well-characterized procedures described in previous studies as cited below. Time points, treatment conditions, and concentrations of pharmacologic agents specific to individual experiments are provided in the respective figure legends. Additional (previously published) details such as antibody epitope sequences, buffer conditions, and explanations of experimental methods can be found in the Supplemental Data.

Materials

Antibodies were either from commercial sources or described previously, and constructs were made using standard methods (details

(H) Analysis of BiP-GFP translocation during acute stress. HeLa cells cotransfected with BiP-GFP and Prl-GFP (a constitutively translocated control) were subjected to 10 μM Tg or 10 mM DTT for 15 min prior to pulse labeling for 15 min. The cytosolic fraction was extracted with digitonin, and the noncytosolic (i.e., translocated) protein was recovered by immunoprecipitation with anti-GFP. Note that the level of translocated BiP-GFP during stress closely parallels Prl-GFP, indicating no obvious translocational attenuation. BiP-GFP translocation relative to Prl-GFP in the same cells was tabulated for three experiments and shown below the gel.

provided in Supplemental Data). CT was prepared as described (Garrison et al., 2005). DTT was from Roche and dissolved in water. Tg, Tm, BFA, MG132, and ALLN were from Calbiochem, dissolved in DMSO or EtOH (BFA), and used at concentrations indicated in the figure legends. Digitonin was from Calbiochem. Immobilized ConA was from Amersham-Pharmacia.

Cell Culture and Biochemical Analyses

HeLa, COS-7, and N2a cells were cultured in DMEM containing 10% FBS at 5% CO_2 and transfected with Effectene (Qiagen) or Lipofectamine 2000 (Invitrogen). Stable cell lines were generated by selection in Zeocin using standard methods (see Supplemental Data). Replating viability assays were performed and quantified by minor modification of published procedures (Marciniak et al., 2004). Pulse-labeling, fractionation, immunoprecipitation, and solubility analyses were performed by minor modifications of published procedures (Fons et al., 2003; Rane et al., 2004; Levine et al., 2005). Exact times and conditions are provided in individual figure legends. Quantification of radiolabeled products utilized a Typhoon Phosphorimager and accompanying software (Molecular Dynamics).

In Vitro Reconstitution and Translation

Translation in reticulocyte lysate and analyses of translocation by protease protection were as before (Fons et al., 2003). Preparation of RM, mRM, LD-RM, rRM, and rRM containing lumenal proteins was as described (Hegde et al., 1998b; Fons et al., 2003; Garrison et al., 2005).

Supplemental Data

Supplemental Data include 11 figures, supplemental notes, Supplemental Experimental Procedures, and Supplemental References and can be found with this article online at http://www.cell.com/cgi/content/full/127/5/999/DC1/.

ACKNOWLEDGMENTS

We are grateful to Martina Alken for providing several constructs, Jesse Yonkovich for performing some of the initial pulse-chase experiments with PrP, Ryen Fons for preparing and characterizing the LD-RM, Aarthi Ashok for comments on this text, and members of the Hegde lab for insightful discussions. This work was supported by the Intramural Research Program of NICHD at the National Institutes of Health.

Received: June 14, 2006
Revised: August 30, 2006
Accepted: October 4, 2006
Published: November 30, 2006

REFERENCES

Besemer, J., Harant, H., Wang, S., Oberhauser, B., Marquardt, K., Foster, C.A., Schreiner, E.P., de Vries, J.E., Dascher-Nadel, C., and Lindley, I.J. (2005). Selective inhibition of cotranslational translocation of vascular cell adhesion molecule 1. Nature *436*, 290–293.

Drisaldi, B., Stewart, R.S., Adles, C., Stewart, L.R., Quaglio, E., Biasini, E., Fioriti, L., Chiesa, R., and Harris, D.A. (2003). Mutant PrP is delayed in its exit from the endoplasmic reticulum, but neither wild-type nor mutant PrP undergoes retrotranslocation prior to proteasomal degradation. J. Biol. Chem. *278*, 21732–21743.

Fons, R.D., Bogert, B.A., and Hegde, R.S. (2003). Substrate-specific function of the translocon-associated protein complex during translocation across the ER membrane. J. Cell Biol. *160*, 529–539.

Garrison, J.L., Kunkel, E.J., Hegde, R.S., and Taunton, J. (2005). A substrate-specific inhibitor of protein translocation into the endoplasmic reticulum. Nature *436*, 285–289.

Grenier, C., Bissonnette, C., Volkov, L., and Roucou, X. (2006). Molecular morphology and toxicity of cytoplasmic prion protein aggregates in neuronal and non-neuronal cells. J. Neurochem. *97*, 1456–1466.

Hegde, R.S., Mastrianni, J.A., Scott, M.R., DeFea, K.A., Tremblay, P., Torchia, M., DeArmond, S.J., Prusiner, S.B., and Lingappa, V.R. (1998a). A transmembrane form of the prion protein in neurodegenerative disease. Science *279*, 827–834.

Hegde, R.S., Voigt, S., Rapoport, T.A., and Lingappa, V.R. (1998b). TRAM regulates the exposure of nascent secretory proteins to the cytosol during translocation into the endoplasmic reticulum. Cell *92*, 621–631.

Hegde, R.S., Tremblay, P., Groth, D., DeArmond, S.J., Prusiner, S.B., and Lingappa, V.R. (1999). Transmissible and genetic prion diseases share a common pathway of neurodegeneration. Nature *402*, 822–826.

Hollien, J., and Weissman, J.S. (2006). Decay of endoplasmic reticulum-localized mRNAs during the unfolded protein response. Science *313*, 104–107.

Jungnickel, B., and Rapoport, T.A. (1995). A posttargeting signal sequence recognition event in the endoplasmic reticulum membrane. Cell *82*, 261–270.

Kim, S.J., and Hegde, R.S. (2002). Cotranslational partitioning of nascent prion protein into multiple populations at the translocation channel. Mol. Biol. Cell *13*, 3775–3786.

Kim, S.J., Rahbar, R., and Hegde, R.S. (2001). Combinatorial control of prion protein biogenesis by the signal sequence and transmembrane domain. J. Biol. Chem. *276*, 26132–26140.

Kim, S.J., Mitra, D., Salerno, J.R., and Hegde, R.S. (2002). Signal sequences control gating of the protein translocation channel in a substrate-specific manner. Dev. Cell *2*, 207–217.

Levine, C.G., Mitra, D., Sharma, A., Smith, C.L., and Hegde, R.S. (2005). The efficiency of protein compartmentalization into the secretory pathway. Mol. Biol. Cell *16*, 279–291.

Ma, J., and Lindquist, S. (2002). Conversion of PrP to a self-perpetuating PrPSc-like conformation in the cytosol. Science *298*, 1785–1788.

Ma, J., Wollmann, R., and Lindquist, S. (2002). Neurotoxicity and neurodegeneration when PrP accumulates in the cytosol. Science *298*, 1781–1785.

Marciniak, S.J., Yun, C.Y., Oyadomari, S., Novoa, I., Zhang, Y., Jungreis, R., Nagata, K., Harding, H.P., and Ron, D. (2004). CHOP induces death by promoting protein synthesis and oxidation in the stressed endoplasmic reticulum. Genes Dev. *18*, 3066–3077.

Mothes, W., Jungnickel, B., Brunner, J., and Rapoport, T.A. (1998). Signal sequence recognition in cotranslational translocation by protein components of the endoplasmic reticulum membrane. J. Cell Biol. *142*, 355–364.

Orsi, A., Fioriti, L., Chiesa, R., and Sitia, R. (2006). Conditions of endoplasmic reticulum stress favor the accumulation of cytosolic prion protein. J. Biol. Chem. *13*, 2067–2078.

Osborne, A.R., Rapoport, T.A., and van den Berg, B. (2005). Protein translocation by the Sec61/SecY channel. Annu. Rev. Cell Dev. Biol. *21*, 529–550.

Oyadomari, S., Yun, C., Fisher, E.A., Kreglinger, N., Kreibich, G., Oyadomari, M., Harding, H.P., Goodman, A.G., Harant, H., Garrison, J.L., et al. (2006). Cotranslocational degradation protects the stressed endoplasmic reticulum from protein overload. Cell *126*, 727–739.

Plath, K., Mothes, W., Wilkinson, B.M., Stirling, C.J., and Rapoport, T.A. (1998). Signal sequence recognition in posttranslational protein transport across the yeast ER membrane. Cell *94*, 795–807.

Rane, N.S., Yonkovich, J.L., and Hegde, R.S. (2004). Protection from cytosolic prion protein toxicity by modulation of protein translocation. EMBO J. *23*, 4550–4559.

Rutkowski, D.T., and Kaufman, R.J. (2004). A trip to the ER: coping with stress. Trends Cell Biol. *14*, 20–28.

Rutkowski, D.T., Lingappa, V.R., and Hegde, R.S. (2001). Substrate-specific regulation of the ribosome- translocon junction by N-terminal signal sequences. Proc. Natl. Acad. Sci. USA *98*, 7823–7828.

Schatzl, H.M., Da Costa, M., Taylor, L., Cohen, F.E., and Prusiner, S.B. (1995). Prion protein gene variation among primates. J. Mol. Biol. *245*, 362–374.

Shan, S.O., and Walter, P. (2005). Co-translational protein targeting by the signal recognition particle. FEBS Lett. *579*, 921–926.

Voigt, S., Jungnickel, B., Hartmann, E., and Rapoport, T.A. (1996). Signal sequence-dependent function of the TRAM protein during early phases of protein transport across the endoplasmic reticulum membrane. J. Cell Biol. *134*, 25–35.

von Heijne, G. (1985). Signal sequences. The limits of variation. J. Mol. Biol. *184*, 99–105.

Wickner, W., and Schekman, R. (2005). Protein translocation across biological membranes. Science *310*, 1452–1456.

Williams, E.J., Pal, C., and Hurst, L.D. (2000). The molecular evolution of signal peptides. Gene *253*, 313–322.

Yoshida, H., Matsui, T., Hosokawa, N., Kaufman, R.J., Nagata, K., and Mori, K. (2003). A time-dependent phase shift in the mammalian unfolded protein response. Dev. Cell *4*, 265–271.

Cell, Volume *127*

Supplemental Data

Substrate-Specific Translocational Attenuation during ER Stress Defines a Pre-Emptive Quality Control Pathway

Sang-Wook Kang, Neena S. Rane, Soo Jung Kim, Jennifer L. Garrison, Jack Taunton, and Ramanujan S. Hegde

Supplemental Notes

1. It is worth noting that the non-translocated species of PrP was not always readily visualized as in Fig. 1, even under conditions of stress when its generation was increased. This is apparently due to the rapid degradation of non-translocated PrP by a proteasome-dependent pathway (Drisaldi et al., 2003, Rane et al., 2004, and Fig. 3 and 4 of this study). Only when pulse-labeling times were minimized (less than ~15 min) and/or the proteasome was simultaneously inhibited during the experiment (e.g., Fig. 1B) was non-translocated PrP reliably observed. This is presumably the reason many previous studies of PrP have not noted this non-translocated population, and why our own experiments using longer pulse-labeling times (c.f., Fig. 2) or immunoblotting often show little or no cytosolic PrP.

2. The decrease in PrP glycosylation during acute stress (Fig. 1A) is compatible with several plausible explanations including: (i) decreased activity of the oligosaccharyl transferase; (ii) decreased access to sites of glycosylation on PrP due to its misfolding; (iii) increased retrotranslocation (and subsequent deglycosylation by cytosolic N-glycanase); (iv) selective degradation of membrane-bound PrP transcript (resulting in selective synthesis of non-targeted mRNA); (v) decreased translocation into the ER. All but the last two of these is effectively ruled out by the demonstration that signal sequence replacement restores glycosylation efficiency under the same stress conditions (Fig. 1B). While it is possible that the piece of mRNA encoded by the PrP signal sequence causes the effects observed, this seems unlikely given that substantial changes to the nucleic acid sequence (without altering the protein sequence) had no effect on stress-dependent changes in PrP biosynthesis (Fig. S2). Thus, the relatively circumscribed role of the signal sequence during the early stages of PrP biosynthesis limits the possible explanations to those involving targeting to the translocon and initiation of translocation. After these steps are completed, the signal sequence is co-translationally removed by signal peptidase by the time ~150 amino acids of PrP are synthesized (Kim and Hegde, 2002), well before the glycosylation sites (at positions 181 and 197) are even synthesized. From this point, the fate of PrP, Prl-PrP, and Opn-PrP are ostensibly equivalent in that they all are translocated into the same ER lumenal environment, encounter the same biosynthetic machinery, and subjected to the same quality control pathways. Although signal sequences can have functions after their removal, no evidence for such a role in PrP biosynthesis has emerged. Similarly, while the choice of signal sequence can influence PrP topology (Rutkowski et al., 2001; Ott and Lingappa, 2004), the alternate

topologic variants represent at most a few percent of the total PrP synthesized in vivo (Hegde et al., 1998a; Kim et al., 2002; Stewart and Harris, 2001). And finally, the examples where signal sequences influence glycosylation directly (Anjos et al., 2002; Rutkowski et al., 2003) are all cases of close juxtaposition of the signal sequence cleavage and glycosylation sites, which is not the case with PrP. Thus, the stress-dependent effect on PrP glycosylation must be due to an event influenced by the signal sequence, which in turn implies it occurs before ~150 amino acids of PrP are synthesized. Hence, the only plausible explanation is a co-translational attenuation of forward translocation into the ER. Based on several in vitro studies, this could be due to either a failure to successfully initiate translocation (Voigt et al., 1996; Fons et al., 2003) or co-translational slippage out of the translocon to the cytosol (Garcia et al., 1988; Ooi and Weiss, 1992; Nicchitta and Blobel, 1993; Hegde and Lingappa, 1996; Hegde et al., 1998b).

3. Although one might have expected the non-translocated glycoproteins generated during ER stress (e.g., Fig. 5C, 5E) or CT treatment (Fig. S7) to be visualized as extra bands in the cytosolic fraction, this is not the case for several reasons. First, most proteins aborted in their translocation have hydrophobic domains that do not allow them to be released efficiently into the soluble cytosolic fraction upon treatment of cells with low concentration of digitonin (e.g., Fig. S3 in the case of PrP). Second, the non-translocated material appears to be rapidly ubiquitinated (perhaps in some cases, co-translationally; Turner and Varshavsky, 2000) and degraded (e.g., Fig. 4A). And third, the relative abundance of radiolabeled cytosolic proteins versus ER-targeted glycoproteins is roughly 5:1, obscuring the detection of non-translocated ER proteins in total cytosolic fractions. Note however that upon immunoprecipitation, non-translocated proteins can indeed be detected in the cytosolic fraction (Fig. S3), albeit at relatively low yield even under conditions where translocation is inhibited completely with CT.

4. To gain insight into the step(s) at which translocation is attenuated during pQC and guide us in its reconstitution in vitro, we employed semi-permeabilized cells in which cytosolic mRNAs, ribosomes, and factors could be separated from membrane-bound components (see Fig. S10A). In this approach, semi-permeabilized cells lacking cytosolic contents are added to an in vitro translation reaction containing ^{35}S-Methionine to complete the translation (i.e., 'read-out') of endogenous mRNAs engaged by membrane-bound ribosomes. The disposition of the radiolabeled products (translocated into the ER or not) can then be assessed using a protease protection assay. Translocational attenuation at the membrane would result in mRNAs being recovered in the semi-permeabilized cells, but failure of their translated products to be successfully sequestered into the ER lumen. By contrast, a targeting defect of a protein would lead to the respective mRNA being cytosolic, therby being lost at the semi-permeabilization step itself. Hence, the protein product would not be generated upon readout of the semi-permeabilized cells. The semi-permeabilization, readout reaction, and ability to effectively remove mRNAs that fail to target to the ER were first tested in control experiments (Fig. S10B).

Upon applying this assay to acutely stressed cells, we observed the readout products from membrane-bound ribosomes to be reduced to ~65% of control cells (Fig. S10C, lanes 1-3). This decrease was uniform among the various proteins visualized by the readout assay (see quantitation of individual bands in Fig. S10D), presumably because translational attenuation prior to semi-permeabilization led to decreased amounts of engaged mRNAs. Upon protease digestion of the membrane-bound readout samples (Fig. S10C, lanes 4-6), we consistently found the degree of overall protection (which reflects translocation into the ER lumen) to be lower (by

~30-40%) for the stressed samples (Fig. S10E). Quantitation of individual bands on the autoradiograph (Fig. S10D) indicated that this overall decrease was an average of some proteins whose level of protection was substantially decreased in the stressed cells and others whose degree of protection was largely unaffected. This effect was even more obvious when the semi-permeabilized cells were re-isolated after protease digestion to remove proteolytic fragments generated from non-translocated products (Fig. S10F). Although some of these differences in protease sensitivity could be due to differences in membrane protein folding and not translocation, this seems unlikely due to the use of very high concentrations (500 μg/ml) of the highly active proteinase K. Thus, the stressed cells appear to show a substrate-specific decrease in translocation by this assay that mirrors results from the analysis of glycoprotein biogenesis in vivo.

Importantly, including a small amount of in vitro synthesized transcript for Prl in the translation reactions led to equal levels of Prl synthesis in stressed and unstressed samples (Fig. S10G). Furthermore, a portion of the exogenously translated Prl was translocated into the ER of the semi-permeabilized cells and subsequently protected from protease. Since Prl translocation and protease protection were equal in all three samples, we could rule out any differences in ER abundance or integrity as the explanation for different degrees and patterns of protease protected translation products in the stressed cells. Hence, although the profile of mRNAs that are targeted to the ER membrane during acute stress are similar (albeit reduced in overall amount) to unstressed conditions, the successful entry of the translated products into the protease-protected space of the ER lumen is diminished for a subset of these proteins. This suggests that the translocation defect in stressed cells that facilitates pQC is likely to be at a post-targeting step (i.e., after the mRNA has arrived at the ER membrane).

5. After solubilization, the reconstitution of proteins into the lumen of rRM to high concentrations has proven to be technically difficult. Unlike membrane proteins that become concentrated in the bilayer upon detergent removal, soluble proteins must rely on becoming trapped in the vesicle during its formation, therby limiting its concentration in the lumen to that present in the solution during reconstitution. Unfortunately, for reasons that are not entirely clear, very high total protein concentrations during the reconstitution procedure seem to interfere with vesicle assembly and recovery. This limits the maximal concentration of proteins achievable in the lumen of rRM to levels well below the normal concentration of lumenal contents (estimated to be at least 100 mg/ml).

6. Although we do not yet understand how changes on the lumenal side of the ER membrane can influence the function of signal sequences that operate largely on the cytosolic face of the ER, several models are plausible. Because lumenal chaperones can interact with translocating nascent proteins early in their synthesis, it is possible that for some substrates, lumenal protein interactions are important to prevent slippage out of the translocon. Such a model is consistent with observations of polypeptide slippage through the translocon (Garcia et al., 1988; Ooi and Weiss, 1992; Nicchitta and Blobel, 1993; Hegde and Lingappa, 1996; Hegde et al., 1998b), a possible gap between the membrane-bound ribosome and translocon (Menetret et al., 2005), and the apparently different affinities among signal sequences for the translocon (Kim et al., 2002). Thus, for some substrates, weakly interacting signals may allow slippage through the ribosome-translocon gap unless the mature domain of the polypeptide interacts with a lumenal chaperone immediately after its exposure to the lumen. Another model involves lumenal chaperones

altering the gating properties of the translocon such that some signals are influence in their ability to productively engage the translocation apparatus. Support for this model comes from the observation that BiP may influence or be part of the lumenal gate of a mammalian translocon (Hamman et al., 1998), and that the gating efficiencies of signal sequences varies among substrates (Kim et al., 2002). And finally, one of more lumenal components could influence the function of an accessory translocon factor (such as TRAM or the TRAP complex) that has already been shown to be required for translocation of selected substrates in a signal sequence-dependent manner (Voigt et al., 1996; Fons et al., 2003).

7. Although the magnitude of translocational attenuation (~30-50%) during acute stress is quite modest, two arguments can be made for its physiological relevance. First, evidence for the importance of even small changes in substrate burden during stress has been provided by recent studies on the role of translational attenuation in mice. Mice that are unable to attenuate translation during acute stress [due to a non-phosphorylatable eIF2α (S51A)] show a severe phenotype in highly secretory tissues (Scheuner et al., 2001). Remarkably however, even mice heterozygous for eIF2α(S51A), capable of at most half the level of translational attenuation compared to wild type mice, nonetheless show a diabetic phenotype ascribed to impaired β-cell function caused by exceeding the folding capability of the ER (Scheuner et al., 2005). Conversely, artificially attenuating translation by either PERK activation or by use of a translational inhibitor can be protective in cell culture models of ER stress and toxicity (Tan et al., 1998; Lu et al., 2004). Thus, in at least some cell types and under some conditions, the ER biosynthetic machinery is working at close to its capacity, making the reduction of substrate burden under stress conditions especially critical to cell viability. By adding a second layer of attenuation that is selective to the site of stress, translocational attenuation may permit the cell to maintain general translation at levels higher than it could otherwise afford. This would allow a higher level of synthesis of any essential non-ER proteins, whose folding and maturation are presumably not compromised during ER stress. The second reason a ~30-50% effect on overall translocation is likely to be significant is because not all substrates are affected uniformly. Especially problematic proteins (whose folding is particularly complex and/or highly dependent on multiple chaperones) may be attenuated to a greater degree than other proteins whose propensity to misfold is minimal. Thus, while the *average* attenuation is modest, the range appears to be broad and substrate-dependent. This may explain why bypassing pQC for a single (especially misfolding-prone) substrate such as PrP can have consequenes for a very general outcome like susceptibility to ER stress. Thus, the degree of translocational attenuation may be commensurate with the overall risk of terminal misfolding in the ER lumen. Similarly, proteins whose entry into the ER is important even during ER stress may not be subject to this type of regulation. Indeed, we have found that BiP (like TRAPα in Fig. 5F), whose upregulation is critical for recovery from and adaptation to stress, maintains a high level of translocation even during maximal acute stress (Fig. 7H).

Supplemental Experimental Procedures

Materials

Antibodies were described previously or from the following sources: TRAPα, Sec61β, and TRAM (Fons et al., 2003); 3F4 mouse monoclonal against PrP (Signet); VCAM1 (Santa Cruz Biotechnologies); GFP (Clontech); BiP (BD Biosciences); PDI and Cnx-N (StressGen). Expression constructs encoding PrP, Prl, Prl-PrP, PrP-Prl, Opn-PrP, PrP-GFP, Prl-PrP-GFP, and VCAM1, have been described (Kim et al., 2002; Fons et al., 2003; Rane et al., 2004; Garrison et al., 2005). The GFP expression construct was from Clontech. The coding regions of Frizzled-7, CRFR, and TRAPα were amplified by PCR and subcloned into a pCDNA3.1-based vector. Prl-CRFR and Opn-Prl were made using a strategy described previously for other signal sequence fusions (Kim et al., 2002). Frizzled-7, CRFR, and Prl-CRFR were each tagged at the C-terminus with an epitope (KTNMKHMAGAAA) recognized by the 3F4 antibody. PrP-mod was made by digesting the PrP expression plasmid with Bgl2 and PflM1 (which flank the signal sequence), and replacing the removed region with synthetic oligonucleotides coding for the sequence in Fig. S2A. Cotransin was prepared as described (Garrison et al., 2005) and dissolved in DMSO. DTT was from Roche and dissolved in water. Tg, Tm, BFA, MG132, and ALLN were from Calbiochem and dissolved in DMSO or EtOH (BFA). Each compound was first tested in preliminary experiments to determine the optimal concentration for each cell type. For BFA, efficacy was judged by dispersal of Golgi in live cells using a fluorescent protein-tagged marker (Mannosidase II; Sciaky et al., 1997). MG132 was used at either 5 μM or 10 μM, concentrations that lead to partial inhibition as judged by the level of cytosolic PrP accumulation (Rane et al., 2004). DTT and Tg were used at concentrations sufficient to induce translational attenuation (a proximal indicator of ER stress) to a level of ~30-70% (see Fig. S1). For HeLa cells, this was 10 mM and 10 μM, respectively. Tm was used at a concentration of 1 μg/ml. DeoxyBigCHAP and Digitonin were from Calbiochem. Digitonin was purified further as described (Gorlich and Rapoport, 1993). Immobilized ConA was from Amersham-Pharmacia and washed into IP buffer (see below) just before use for capture of glycoproteins.

Cell Culture

HeLa, Cos-7, and N2a cells were cultured in DMEM containing 10% FBS at 5% CO_2. HeLa cells were transfected with Effectene (Qiagen); N2a cells were transfected with Lipofectamine 2000 (Invitrogen). Stable cell lines were generated by selection in Zeocin for 4 weeks, followed by subcloning of individual colonies. Several individual clones at different expression levels were analyzed. Data are shown for two clones whose levels of expression and growth rates were the same. Replating viability assays were performed on cells in either 96-well dishes or 35 mm dishes. Following the treatments, cells were trypsinzed, collected, sedimented, and resuspended in fresh media. The total number of viable cells were counted in a hemocytometer using trypan blue. Equal numbers of cells for each condition (usually between 2,500 and 10,000) were plated into 10 cm dishes, and allowed to grow for between 8 and 10 days before fixation in methanol and staining with crystal violet. To quantify the results, the plates were digitized using a flatbed scanner, and a threshold function applied to convert images to black colonies on a white background. The total number of black pixels on each plate (which takes into account colony number and colony size) was measured and used to determine relative growth. It should be noted that all experiments shown in any panel were performed in parallel. Results from experiments performed on different days were not compared because of variations in growth and culture

conditions (note for example, the differences in colony size and number among different experiments). However, we confirmed in multiple independent experiments (at least three) that the *relative* differences shown in the figures were consistently observed. For the re-plating assays (Fig. 4C), treated cells from a 35 mm dish were trypsinized and replated with fresh media into 96-well plates which were allowed to grow for up to 72 h before harvesting and analysis by immunoblots. Immunofluorescence staining with 3F4 anti-PrP and confocal microscopy was as previously described (Rane et al., 2004).

Labeling and Biochemical Analyses of Cultured Cells

Pulse-labeling was performed on cells pre-incubated for 30 min in serum-free media lacking methionine and cysteine, to which Translabel (MP-Biomedical) was added at a concentration of 200 μCi/ml to initiate the labeling. Chase was carried out in complete media lacking label. Cells were harvested for immunoprecipitation in 1% SDS, 0.1 M Tris, pH 8, boiled, and diluted 10-fold in IP buffer (50 mM Hepes, pH 7.4, 100 mM NaCl, 1% Triton X-100) prior to addition of antibodies. Fractionation of cytosolic from non-cytosolic proteins using selective extraction with digitonin (Fig. S3A) was as before (Levine et al., 2005). Each fraction was subsequently immunoprecipitated using antibodies against GFP. Solubility assays for PrP were as described (Rane et al., 2004). Fractionation of cytosolic and glycoproteins (by the scheme shown in Fig. 5A) was performed on cells growing and labeled in 35 mm dishes. Cells were first washed in 1 ml PBS and extracted on ice with 1 ml KHM buffer (110 mM KAc, 20 mM Hepes, pH 7.2, 2 mM MgAc2) containing 150 ug/ml digitonin for 5 min. The cytosolic extract was reserved, and the remaining material was washed once in KHM and subsequently extracted in 1ml IP buffer to recover the non-cytosolic proteins. The glycoproteins were recovered from the non-cytosolic fraction by incubation for 1 h with 50 ul packed ConA beads, followed by washing 3 times in IP buffer, and elution for 1 h at room temperature in 350 ul IP buffer containing 0.25 M α-methyl-D-mannopyranoside. Aliquots of the cytosolic extract and eluted glycoproteins were analyzed directly on SDS-PAGE and autoradiography. Quantification of radiolabeled products utilized a Typhoon phosphorimager and accompanying software (Molecular Dynamics). All gels were also stained with coomassie blue to confirm equal recovery and loading of total proteins, glycoproteins, and IgG (in the case of immunoprecipitations). Any experiments where recovery was not uniform for all samples were not analyzed. This ensured that any differences in radiolabeled products were not a consequence of technical variability.

Analysis and Modulation of Chaperones in Cultured Cells

For biochemical analysis of chaperones, cells in 35 dishes were treated as indicated in the legend to Fig. 7, transferred to ice, and pre-extracted with KHM containing 150 μg/ml digitonin and 10 U/ml apyrase for 5 min followed by a wash in KHM containing 10 U/ml apyrase. This led to removal of cytosolic contents and depletion of ATP levels. The remaining cellular material was then solubilized by scraping into 250 ul of 50 mM Hepes, pH 7.4, 100 mM NaCl, 2 mM MgCl2, 0.5% Triton X-100. The lysate was centrifuged for 5 min at 10,000 rpm in a microcentrifuge and the supernatant removed as the ‘soluble’ fraction. The pellet was dissolved in SDS-PAGE sample buffer and referred to as the ‘insoluble’ fraction. The soluble fraction was either analyzed directly in some cases or 200 ul of it was applied to a 2ml linear 5%-25% sucrose gradient prepared in the Triton X-100 lysis buffer above. After centrifugation for 3 h at 55,000 rpm in a TLS-55 rotor (Beckman), 200 ul fractions were collected from the top and analyzed by SDS-PAGE and immunoblotting as indicated in the Figure legends. For pre-conditioning, cells were

treated with 10 mM DTT for 1 h followed by replacement with fresh media and recovery for 16 h.

In Vitro Translation and Readout Analyses

Readout assays on semi-permeabilized cells (Fig. S10) were carried out on cells grown in 35 mm dishes. The cells were placed on ice, semi-permeabilized with 100 ug/ml digitonin in KHM for 5 min, and the digitonin extract removed. The cells remaining on the dish were rinsed once in KHM buffer, scraped into 2 ml KHM, isolated by sedimentation for 2 min at 1000 rpm in a microcentrifuge, and resuspended in 10 ul KHM. The semi-permeabilized cells were used immediately (at a concentration of 2.6 ul per 25 ul total reaction volume) in translation reactions containing rabbit reticulocyte lysate. Translations were for 30 min at 32°C. Where indicated, in vitro synthesized transcripts coding for control proteins were included in the translation reaction. Translation reactions were divided into two aliquots on ice, one of which was digested with proteinase K (PK) at 0.5 mg/ml for 1 h. The reactions were terminated with 5 mM PMSF and transferred directly to 10 volumes of boiling 1% SDS, 0.1 M Tris, pH 8. Alternatively (Sup. Fig. S10F), the protease-digested cells were re-isolated by centrifugation and dissolved directly in SDS-PAGE sample buffer. To analyze cytosolic ribosomes (Supl. Fig. S10F), the cytosolic extract after digitonin treatment was centrifuged at 70,000 rpm for 30 min in a TLA100.3 rotor and the mRNA-bound ribosomal pellet was resuspended in 10 ul KHM. This was added to translation reactions as above. Quantification of the radiolabeled products utilized a phosphorimager.

Membrane Fractionation and Reconstitution

RM were prepared as described (Walter and Blobel, 1983). LD-RM were prepared as described in Garrison et al., 2005: 100 ul RM at a concentration of 1 eq/ul in membrane buffer (50 mM Hepes, pH 7.4, 250 mM sucrose, 1 mM DTT), were diluted with four volumes of membrane buffer containing 0.075 % DeoxyBigCHAP on ice. After 10 min on ice, the microsomes were sedimented at 100,000 rpm for 15 min at 4°C in a TL100.3 rotor. The supernatant was removed, and the tube was carefully rinsed (without disturbing the pellet) twice with 500 ul of membrane buffer (lacking detergent). The pellet was resuspended in 500 ul of the membrane buffer (lacking detergent), transferred to new tubes, and sedimented again as above. After removing the supernatant, the membranes were resuspended in 100 ul. mRM were prepared exactly as above and in parallel, but without detergent in any of the buffers. Serial dilutions of mRM and LD-RM were analyzed on a single gel and immunoblotted with BiP and PDI to estimate the degree of lumenal protein depletion, which proved to be ~80-90%. To prepare rRM, we used the method described in Fons et al., 2003: RM (at a concentration of 1 eq/ul in membrane buffer) were first pre-extracted by dilution with an equal volume of membrane buffer containing 2% saponin. After 5 min on ice, the membranes were isolated by sedimentation (100,000 rpm for 15 min at 4°C in a TL100.3 rotor) and resuspended in extraction buffer (350 mM KAc, 50 mM Hepes, 5 mM MgAc2, 15% glycerol) in the original volume. After addition of DeoxyBigCHAP to 0.8% and incubation on ice for 10 min, the insoluble material was removed by centrifugation (100,000 rpm for 30 min at 4°C in a TL100.3 rotor), and the detergent extract reconstituted into proteoliposomes by detergent removal as previously described (Fons et al., 2003). The pre-extraction step above removes ~90% of lumenal proteins, while the reconstitution and re-isolation procedure removes essentially any remaining lumenal proteins. We estimated rRMs to contain less than 2% of lumenal contents relative to RM. To reconstitute rRM with lumenal

proteins (Hegde et al., 1998b), a lumenal protein extract was prepared by extracting RM (at 1 eq/ul in membrane buffer) with an equal volume of 0.25% Digitonin in membrane buffer. After removing the membranes, the lumenal protein fraction was precipitated by adjusting the sample to 13% PEG-6000. The protein precipitate was collected by centrifugation in a microcentrifuge, and dissolved in extraction buffer in one-twentieth the original volume of starting RM. For co-reconstitution, this concentrated lumenal protein fraction was added in varying amounts to the membrane protein extract above and reconstituted into proteoliposomes by detergent removal as before (Fons et al., 2003). In vitro translation and translocation assays and determination of translocation by protease protection were performed as described previously (Fons et al., 2003).

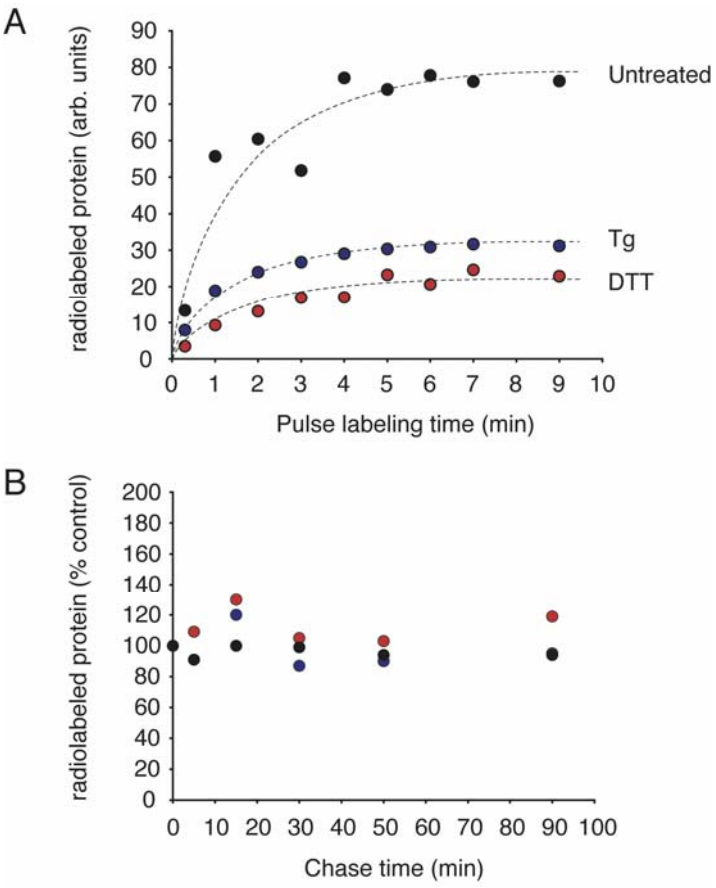

Figure S1. Relative Rates of Protein Synthesis and Degradation during Acute ER Stress

(A) Cultured Hela cells in 96-well dishes were pulse-labeled with [35]S-Methionine for the indicated times before quantification of total radiolabeled proteins by SDS-PAGE and phosphorimaging. Cells contained either no stressor (black symbols), Tg (blue symbols), or DTT (red symbols) during the entire experiment. The saturation of labeled protein after ~5 min in this experiment raised the possibility that non-linear kinetics of labeling could influence the quantification of some experiments. However, this concern can be mitigated by three observations. First, we have done experiments in which the labeling was for only 5 min and observe the same results as with longer labeling times (data not shown). Second, when using larger culture dishes (as is the case in nearly all experiments shown in the main text), incorporation of label was confirmed to be linear for at least 30 min (suggesting that this saturation effect may be due to the 96-well plate format). And third, even in experiments where incorporation is non-linear, the same kinetics are observed for both untreated and stressed cells, making it very unlikely that differences between them can be explained by the labeling alone.

(B) After pulse-labeling Hela cells in 96-well plates for 10 min as in panel A, the labeling media was replaced with unlabeled media and chased for the indicated times before quantitative analysis of total radiolabeled protein by SDS-PAGE and phosphorimaging. The data are normalized to the amount of radiolabeled protein present immediately after the pulse labeling (defined as time 0). Cells contained either no stressor (black symbols), Tg (blue symbols), or DTT (red symbols) during the entire experiment.

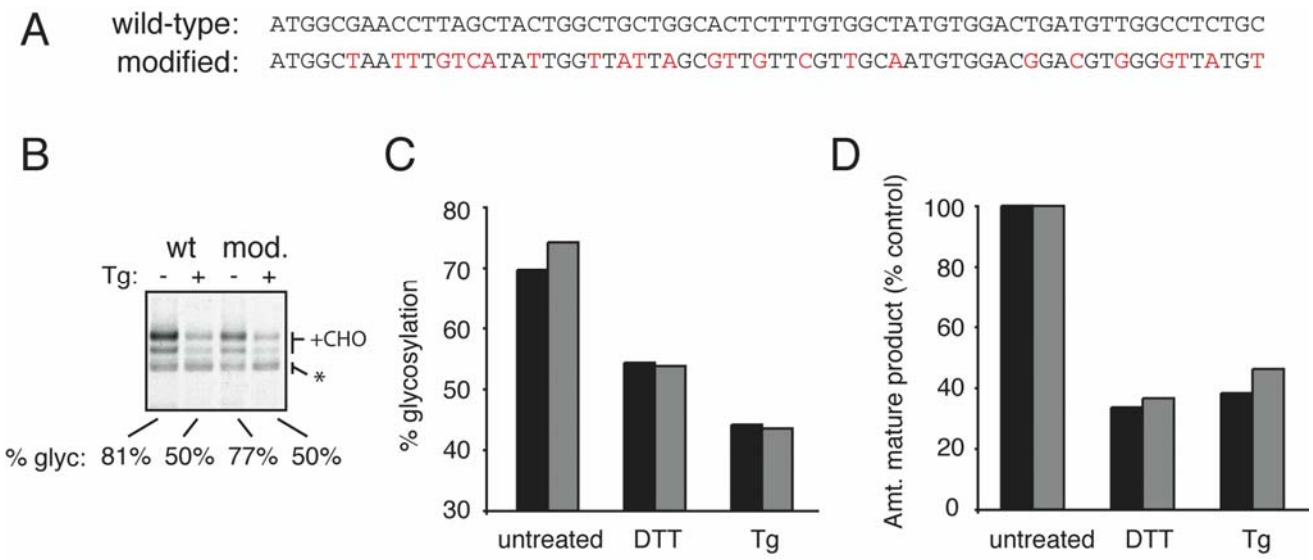

Figure S2. Effect of Nucleotide Changes in the Signal Sequence on PrP Biosynthesis

(A) Nucleotide sequences of the wild type PrP signal sequence and a modified version coding for the same protein sequence. Differences are indicated in red.

(B) The wild type and modified versions of PrP were analyzed for stress-dependent effects on their biosynthesis as in Fig. 1A. Note that in both cases, Tg stress causes a significant and comparable reduction in translocation as judged by decreased glycosylation. The positions of the glycosylated ('+CHO') and non-glycysylated ('*') species are indicated. A similar effect was observed with DTT stress (not shown).

(C) The degree of stress-dependent reduction in PrP glycosylation is plotted for the wild type (black bars) and modified (grey bars) versions of PrP.

(D) The reduction in generation of fully glycosylated mature PrP during acute stress was quantified as in Fig. 1A and normalized for the degree of overall translational attenuation. Note that during acute stress, the generation of fully glycosylated PrP is reduced to ~40% of what could be expected on the basis of translational attenuation alone. This effect was similar for both wild type PrP (black bars) and modified PrP (grey bars), suggesting that it is not influenced by changes in the nucleotide sequence of the signal sequence.

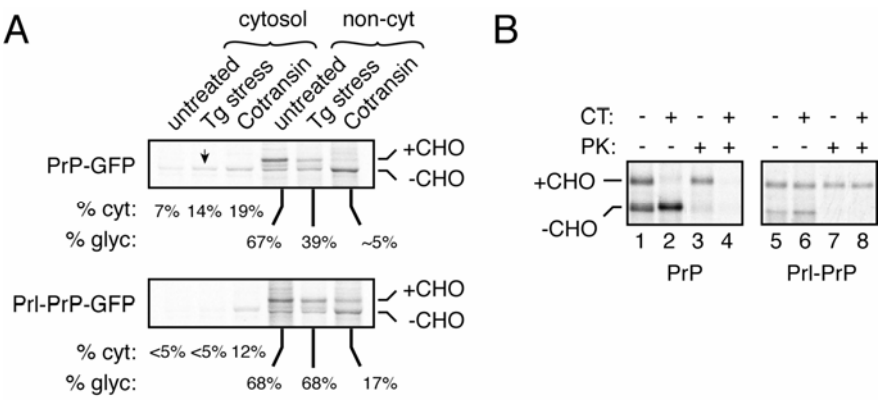

Figure S3. Analysis of PrP Translocation by Cell Fractionation

Cell fractionation experiments to directly demonstrate the cytosolic disposition of non-glycosylated PrP were confounded by its relative insolubility and propensity to aggregate (Ma and Lindquist, 2002; Drisaldi et al., 2003; Rane et al., 2004; Grenier et al., 2006). However, a GFP-tagged version of PrP (PrP-GFP) proved somewhat more amenable to fractionation and displayed the same selective reduction in translocation (as judged by decreased glycosylation) during acute ER stress as untagged PrP (panel A). At least a portion of unglycosylated PrP-GFP could now be observed in the cytosolic fraction, and this species increased (~ 2-fold) during acute stress (arrowhead, panel A). Importantly, the translocation efficiency of Prl-PrP-GFP was not changed significantly during stress, and it was not observed in the cytosolic fraction under either normal or stressed conditions (Panel A). Direct inhibition of PrP-GFP translocation with the translocational inhibitor Cotransin (CT; Garrison et al., 2005; see panel B) resulted in no translocation of PrP-GFP (and reduced translocation of Prl-PrP at this concentration in vivo), and increased amounts recovered in the cytosolic fraction. Note however that even when translocation is completely inhibited, only ~20-30% of PrP-GFP could be recovered in a soluble state in the cytosol, probably because the uncleaved hydrophobic domains at the N- and C-terminus of PrP-GFP complicate its efficient fractionation (Rane et al., 2004; our unpublished observations). This technical limitation notwithstanding, these results provide direct corroboration that PrP translocation is selectively reduced during acute ER stress in a signal sequence-dependent manner.

(A) The biosynthesis of PrP-GFP and Prl-PrP-GFP was analyzed by immunoprecipitation of pulse-labeled (30 min) and fractionated HeLa cells acutely treated with 10 μM Tg or 10 mM Cotransin for 30 min. The percent of total synthesized product that is in the cytosolic fraction ('% cyt') or glycosylated ('% glyc') is indicated. Glycosylated ('+CHO') and non-glycosylated ('-CHO') bands are indicated.

(B) PrP and Prl-PrP were translated and translocated in vitro using rough microsomal membranes in the presence or absence of 10 μM CT. Translocation of the products was assessed by a protease protection assay using proteinase K (PK). The unglycosylated ('-CHO') and glycosylated ('+CHO') forms are indicated. Note that CT inhibits translocation of PrP more potently than Prl-PrP, as evidenced by the lack of PrP glycosylation (lane 2) and protease protection (lane 4) in the presence of CT. At higher concentrations, some inhibition of Prl-PrP was observed. Since CT is more potent in vivo than in vitro (Garrison et al., 2005), this partial effect on Prl-PrP was easier to observe in some experiments than others (e.g., as in panel A above).

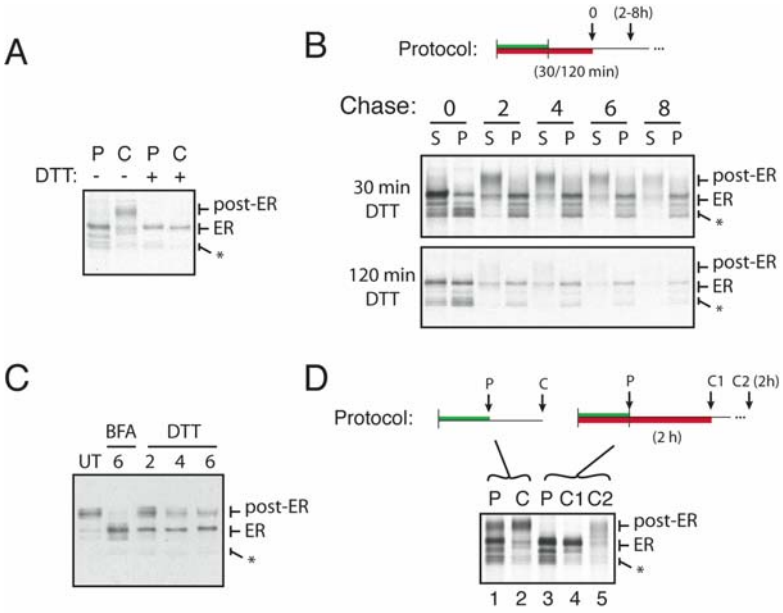

Figure S4. Analysis of PrP Trafficking during DTT and Brefeldin A (BFA) Treatment

(A) Cells transiently transfected with PrP were pulse labeled for 15 min ('P') and chased ('C') in the absence of label for 1 h. The entire pulse-chase was performed in the presence or absence of DTT. Unglycosylated ('*'), core-glycosylated ('ER'), and complex glycosylated ('post-ER') forms of PrP are indicated. Note that PrP, which contains two cysteines that need to be disulfide bonded to fold properly, is retained in the ER in the presence of ongoing DTT stress.

(B) Cells pulse-labeled for 30 min (green bar) were maintained in DTT (red bar) for 30 or 120 additional minutes before return to normal medium and collection of chase time points from 0 to 8h. Each sample was analyzed by solubility assays, immunoprecipitation, and autoradiography as in Figure 2A.

(C) Cells expressing PrP were treated with either DTT or BFA for up to 6 h before analysis by immunoblots. Note the accumulation of the ER form of PrP when ER-to-Golgi trafficking is prevented by BFA. The same form accumulates with DTT, albeit to a lesser extent due to translational and translocational attenuation during this time period.

(D) Cells were pulse-labeled for 30 min in the presence of BFA (lane 3), chased for 2 h without label (but in the presence of BFA; lane 4), and chased an additional 2 h after removal of BFA (lane 5). A pulse-chase in the absence of BFA is shown for comparison (lanes 1, 2). A schematic of the experiment is shown above the autoradiograph, with the period of labeling indicated in green and the period of BFA treatment indicated in red. Unglycosylated ('*'), core-glycosylated ('ER'), and complex glycosylated ('post-ER') forms of PrP are indicated. Note that even after being held in the ER for two hours with BFA, PrP is capable of trafficking to post-ER compartments. The incomplete maturation of its glycans is likely a consequence of trafficking through the Golgi simultaneously with Golgi re-assembly upon BFA removal.

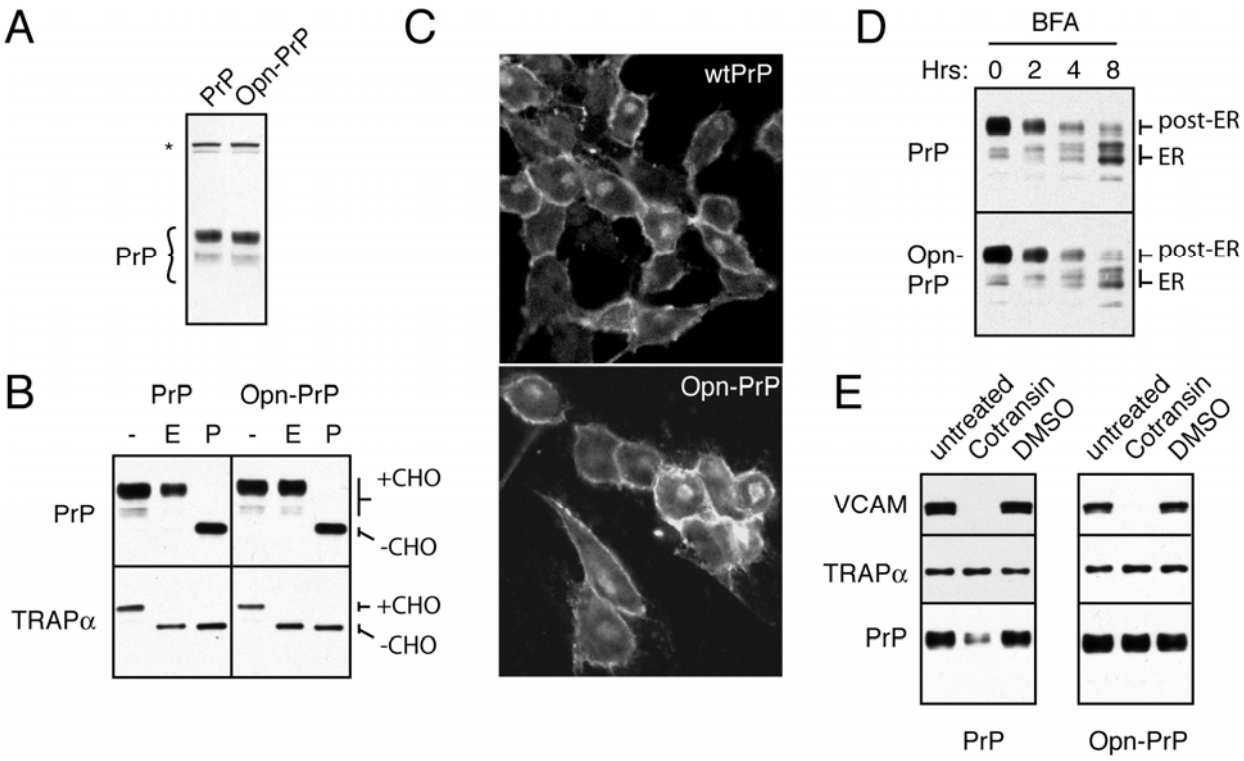

Figure S5. Characterization of PrP and Opn-PrP Cell Lines

(A) Immunoblot of expression levels in stable PrP and Opn-PrP cells. The background band ('*') serves as a loading control.

(B) Lysates from PrP and Opn-PrP cells were treated with Endoglycosidase H ('E') or PNGase F ('P') before immunoblotting for PrP and the resident ER glycoprotein TRAPa. The positions of glycosylated ('+CHO') and unglycosylated ('-CHO') species are indicated.

(C) Immunofluorescence detection of PrP and Opn-PrP in the respective stable cell lines.

(D) Cells stably expressing PrP or Opn-PrP were treated with BFA for the indicated times before analysis by immunoblot. The ER-retained forms of PrP accumulate at the same rate for PrP and Opn-PrP, indicating that in the absence of acute ER stress, the translocation efficiency of both proteins is essentially indistinguishable. Also note that BFA treatment leads to a variable degree of heterogeneity of the PrP glycoforms that accumulate in the ER over time, presumably due to the mixing of Golgi enzymes with the ER compartment.

(E) Cells stably expressing either PrP or Opn-PrP were transiently transfected with a VCAM1 expression plasmid and treated with CT (5 μM) for 8 h before analysis by immunoblots. PrP is inhibited by CT, while Opn-PrP is largely resistant to inhibition at this concentration. VCAM1 is inhibited equally in both cell lines, demonstrating that the resistance of Opn-PrP to CT is due to the signal sequence, and not an inherently resistant cell line. Opn-PrP was inhibited to a greater extent at higher concentrations of CT (~50% inhibition at 20 μM; data not shown).

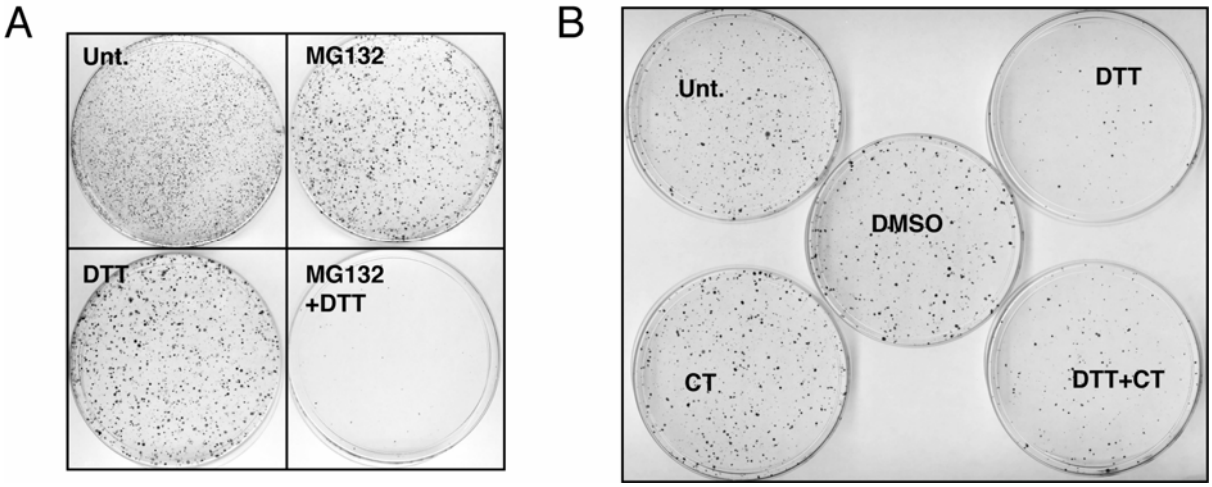

Figure S6. Colony Formation Assays for Cell Survival under Various Conditions

(A) PrP-expressing cells treated with DTT, MG132, or both agents for 18 h were re-plated in normal media and visualized 8 d later by staining with crystal violet.

(B) Opn-PrP expressing cells were treated with the indicated agents for 6 h before re-plating in normal media and visualization 8 d later by staining with crystal violet.

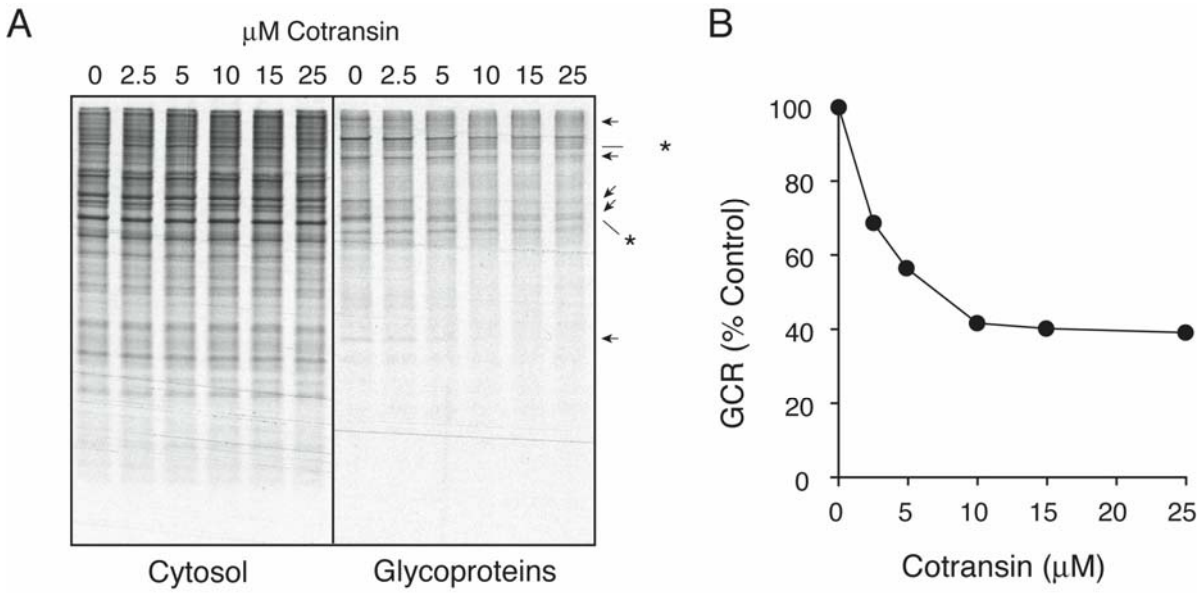

Figure S7. Characterization of Assay for Translocational Attenuation

(A) Cells pulse-labeled for 30 min with increasing concentrations of CT were separated into cytosolic and glycoprotein fractions and analyzed by autoradiography. Note that the glycoprotein samples are from a longer exposure of the film than cytosolic samples. The arrows point to bands that are reduced to varying degrees by CT (presumably due to inhibition of their translocation), while asterisks indicate bands that are largely refractory to CT. Note that no cytosolic proteins are affected by CT. Also, glycoproteins inhibited in their translocation by CT are not easily visualized in the cytosolic fraction for various reasons that are discused in Sup. Note 3.

(B) Ratio of total radiolabeled glycoprotein to cytosolic protein ratio (GCR) quantified from panel A, with the value from untreated cells arbitrarily set to 100%.

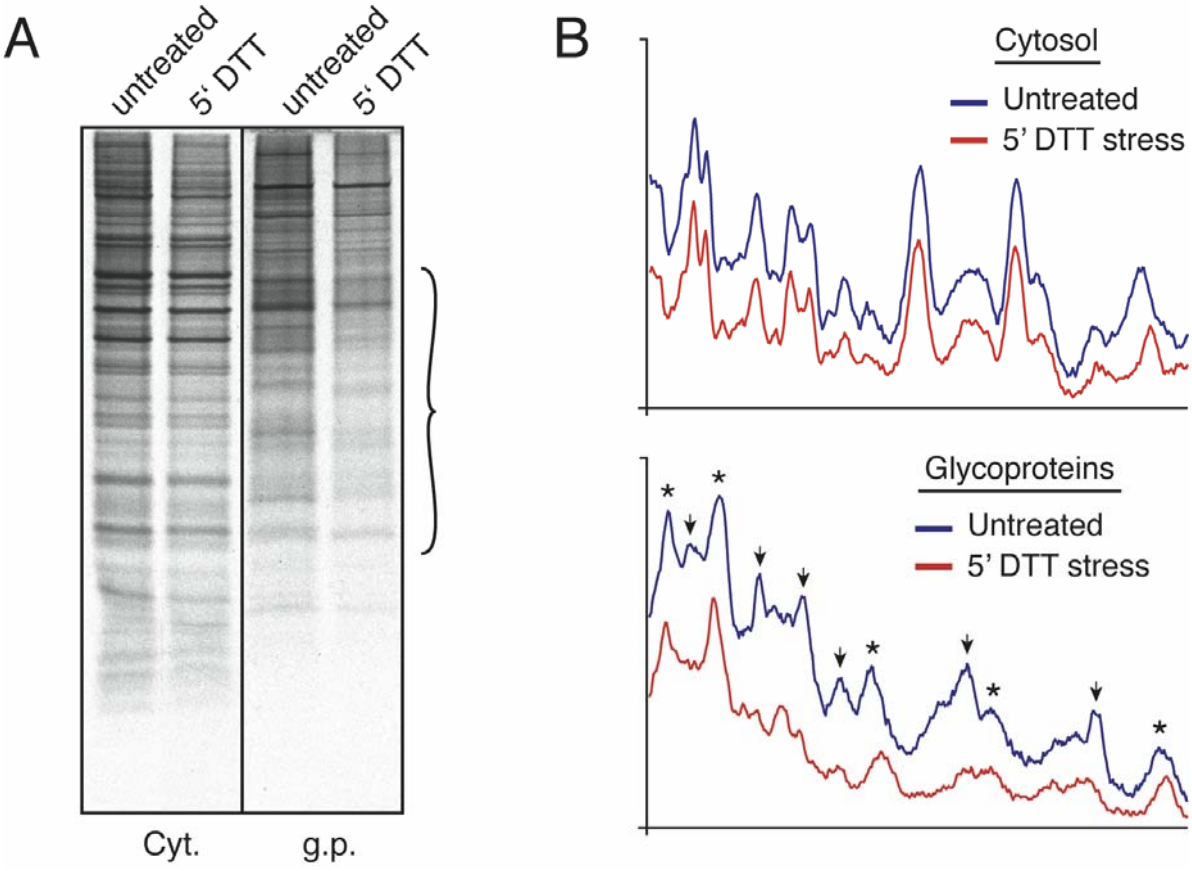

Figure S8. Profiles of Cytosolic Proteins and Glycoproteins during Acute ER Stress

(A) Cultured cells were left untreated or treated for 5 min with 10 mM DTT before pulse-labeling for 5 min and fractionation into cytosolic proteins and glycoproteins. The autoradiograph of newly synthesized cytosolic proteins and glycoproteins is shown at left. The region indicated by the bracket was analyzed by densitometry in panel B.

(B) Densitometry profiles from ~60 kD (left) to ~25 kD (right) of radiolabeled cytosolic proteins (top graph) and glycoproteins (bottom graph) from untreated and DTT-treated cells from panel A. Note that cytosolic proteins uniformly decrease during DTT treatment (due to translational attenuation), while the glycoproteins are reduced to variable levels. Arrows indicate bands that decrease substantially more than that attributable to translational attenuation, while asterisks indicate bands whose decrease is comparable to the level of translational attenuation. It should be noted that some of the changes to the profile of bands could be due to alterations in glycosylation efficiencies at some consensus sites in the presence of 10 mM DTT. However, the overall decrease in glycoproteins is not likely to be due solely to such an effect because a similar decrease was also observed in the presence of Tg (e.g., Fig. 5D), and because this effect was largely reversible depsite the presence of 10 mM DTT in cells preconditioned with an earlier stress (see Fig. 7F).

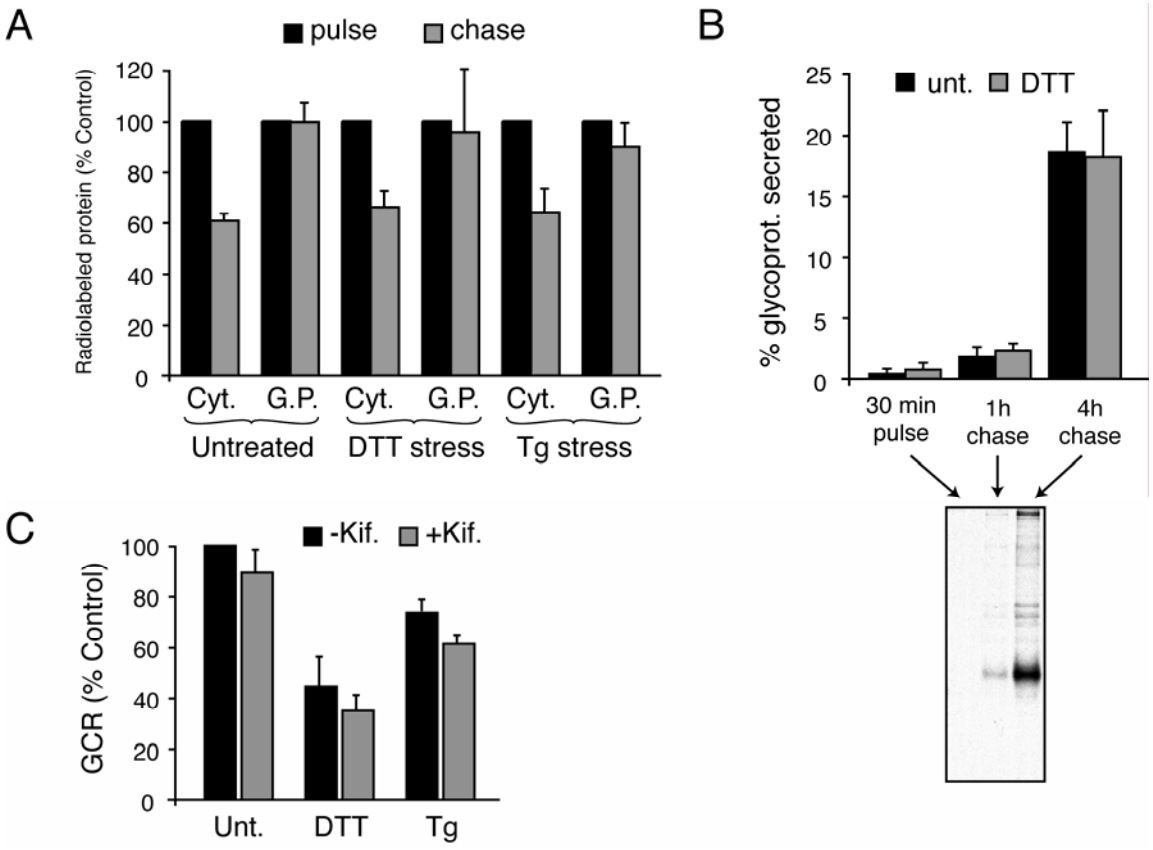

Figure S9. Decreased GCR during Acute ER Stress Is Not Due to Increased Degradation

(A) Total radiolabeled cytosolic proteins and glycoproteins were quantified after pulse-labeling (15 min) and chase in unlabeled media (1 h). Each chase value was normalized to its respective pulse value. Cells were either untreated, exposed to DTT, or exposed to Tg during the entire pulse and chase. The mean ± SD for three replicates is shown. Note that regardless of the treatment condition, ~40% of cytosolic proteins are degraded during the 1 h chase, while very little glycoproteins are lost to either degradation or secretion (see panel B).

(B) Cells were subjected to a 30 min pulse label followed by chase in unlabeled media for either 1h or 4h. The pulse-chase was performed on either untreated (black bars) or DTT-treated cells (grey bars). The radiolabeled glycoproteins in the cell lysate and media were captured by Con A, analyzed by SDS-PAGE, and quantified by phosphorimaging. The percent of radiolabeled glycoproteins secreted into the media is plotted (mean ± SD for three replicates), with a representative autoradiograph for the untreated samples shown below the graph. Note that less than 3% of synthesized glycoproteins are secreted into the media in the first hour.

(C) GCR from untreated or acutely stressed (30 min) cells was determined in the presence or absence of Kifunensine to inhibit access of glycoproteins to the ER-associated degradation (ERAD) pathway. The mean ± SD for three replicates is shown. Note that the GCR decrease during acute stress is the same in the presence or absence of Kifunensine, suggesting that increased ERAD is not involved in changes to the GCR.

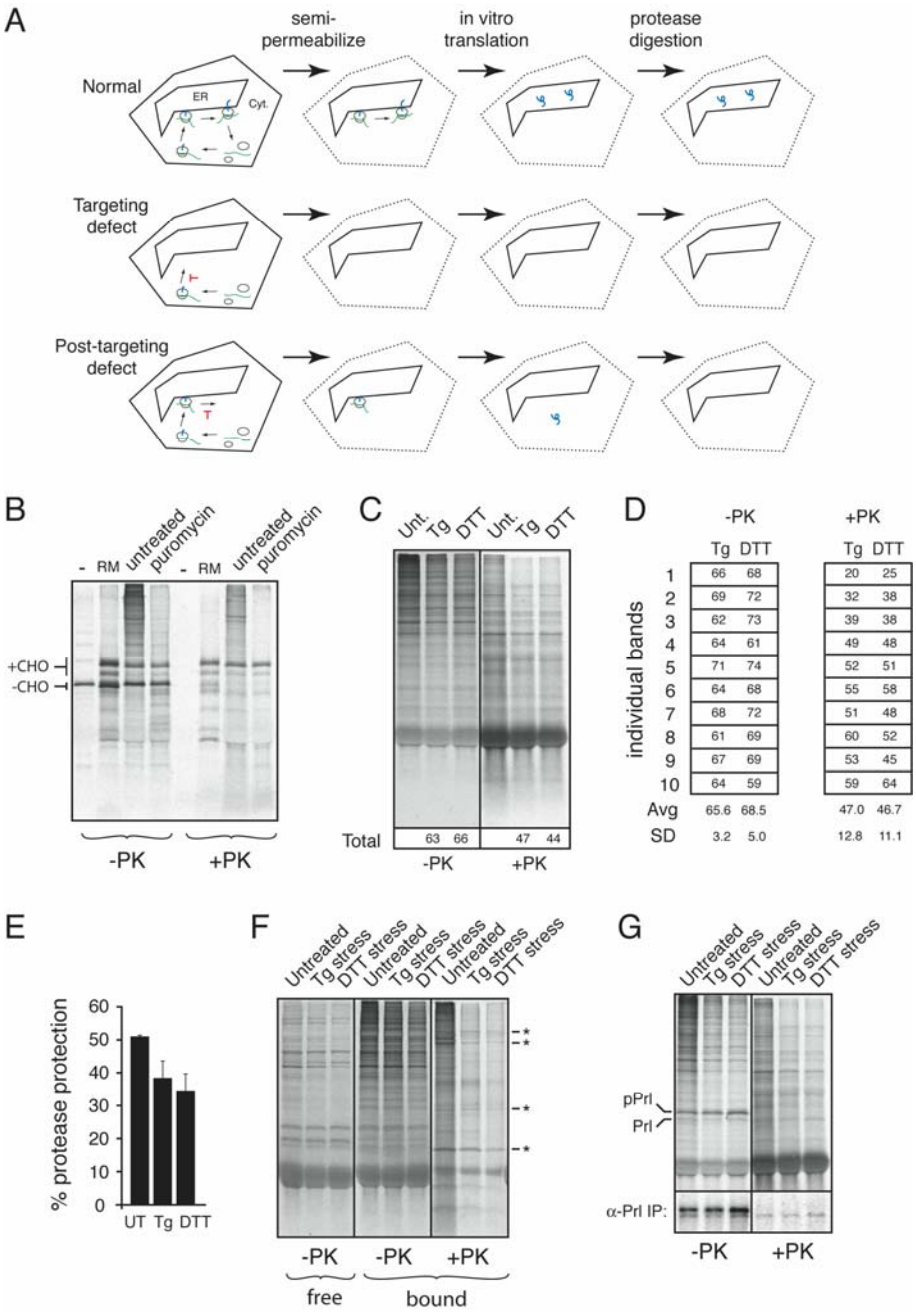

Figure S10. A Posttargeting Step Is Involved in Translocational Attenuation

(A) Experimental design of an assay to distinguish targeting from post-targeting mechanisms of translocational attenuation. Cultured cells are semi-permeabilized with digitonin to remove cytosolic contents including free ribosomes, and the permeabilized cells added to an in vitro translation reaction containing [35]S-Methionine to complete the translation (i.e., 'read-out') of mRNAs engaged by membrane-bound ribosomes. The location of these radiolabeled readout products is assessed by a protease protection assay. A defect in targeting or translation in the cells would manifest as a loss of membrane bound mRNAs, resulting in reduced or no readout products. By contrast, a defect at the level of translocation would permit recovery of membrane-bound mRNAs and their subsequent translation, but result in their accessibility to protease digestion.

(B) In vitro translation reactions containing transcript for PrP was carried out in the presence of: no additions ('-'), pancreatic rough microsomes ('RM'), semi-permeabilized cells ('untreated'), or cells pre-treated with puromycin (200 uM for 15 min) prior to semi-permeabilization ('puromycin'). Note that PrP is synthesized at comparable levels in all reactions. In the presence of either RM or semi-permeabilized cells, PrP is translocated into the ER lumen, as judged by its glycosylation ('+CHO') and protection from proteinase K (PK) digestion. In the untreated semi-permeabilized cells, numerous readout products are generated, which are protected to varying degrees from PK digestion. By contrast, the puromycin-pretreated semi-permeabilized cells generate substantially less readout products due to the loss of membrane-bound mRNAs under these conditions (see panel A).

(C) Cells treated as indicated were semi-permeabilized and the mRNAs engaged by membrane-bound ribosomes were allowed to complete synthesis in vitro. The samples were then subjected to proteinase K (PK) digestion and an aliquot of the total radiolabeled products before and after PK were visualized by autoradiography. The total radiolabeled products in the Tg and DTT lanes were quantified (% relative to untreated lane) and indicated below the respective lanes.

(D) Individual bands in the Tg and DTT lanes (arbitrarily denoted "1" through "10") were quantified (% relative to the same band in the untreated lane) and shown in the table. The average (Avg) and SD of the ten bands are also shown. Note that the level of reduced synthesis (in the -PK lanes) is very similar for all bands, while the degree of protease protection is substantially more variable from band to band (as indicated by the larger SD).

(E) The overall degree of protease protection (of all readout products) from four independent experiments as in panel C were tabulated (mean ± SD).

(F) Readout reactions were performed using semi-permeabilized cells that were pre-treated (before permeabilization) with either nothing ('untreated'), Tg, or DTT for 30 min. After PK digestion, the cells were re-isolated by sedimentation to remove proteolytic fragments. Note that with Tg or DTT, many products are not protected from PK digestion as efficiently as in untreated cells, indicative of their reduced translocation efficiency. The asterisks identify several proteins whose protection is not significantly affected by DTT or Tg, and hence appear to be constitutively translocated at the same efficiency as in untreated cells. In addition, non-membrane-bound (i.e., 'free') ribosomes isolated from the cytosolic extract generated by semi-permeabilization was also subjected to readout analysis. Note that the amount of radiolabeled readout products is reduced to comparable degrees with Tg and DTT for both the free and membrane-bound reactions, indicating that translational attenuation affects both populations uniformly.

(G) A readout reaction exactly as in panel D was performed in the presence of an in vitro generated transcript coding for Prl. The position of the precursor (pPrl) and processed forms of Prl are indicated. An aliquot of the samples was subjected to immunoprecipitation with anti-Prl antisera and the products are shown in the bottom panel. Note the equal levels of Prl synthesis, processing, and protease-protection in all three samples.

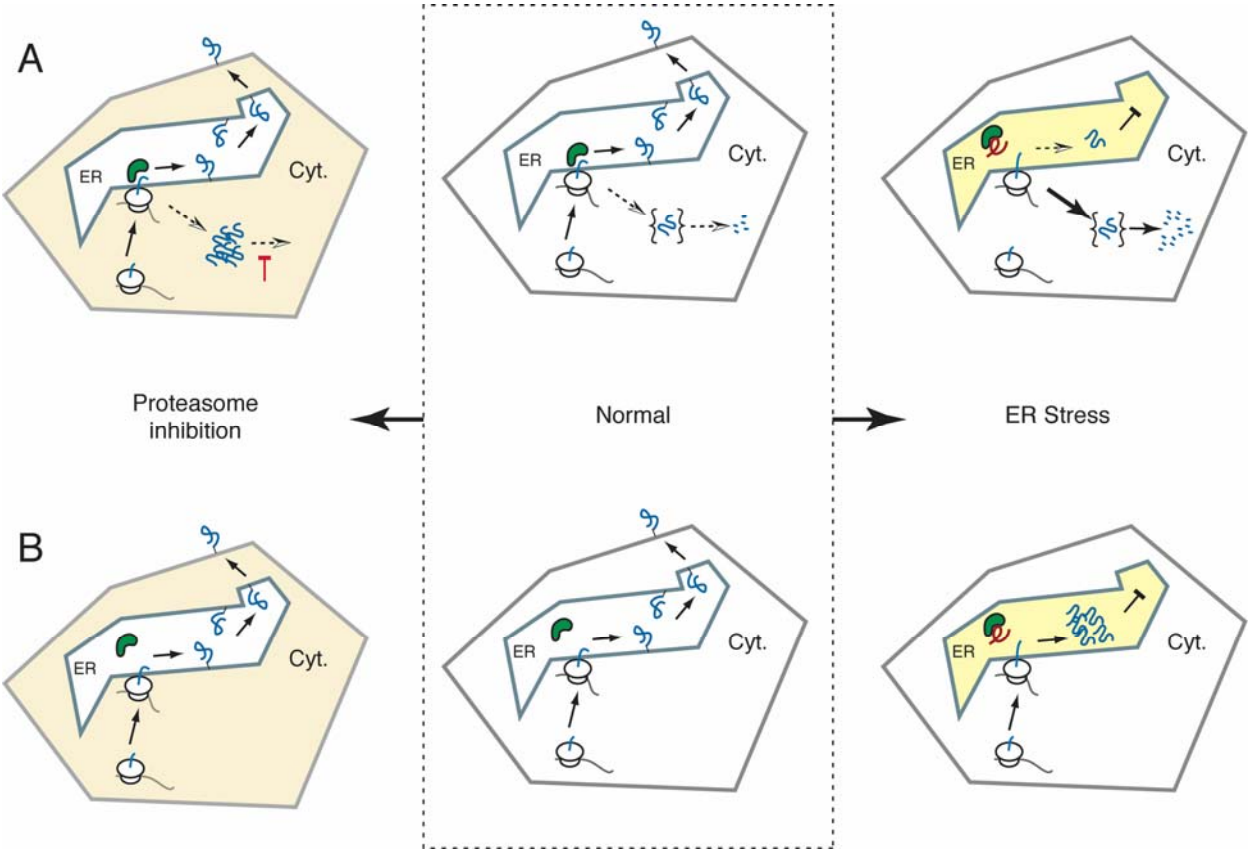

Figure S11. The Role of Translocational Attenuation in Protection from ER Stress

A translocationally attenuatable substrate (such as PrP) versus a constitutively translocated version (such as Opn-PrP) are shown in panels A and B, respectively. The center diagrams show normal targeting, maturation, and traffic to the cell surface for both substrates, with PrP translocation being at least partially dependent on the availability of yet unidentified lumenal factor(s) (e.g., BiP) indicated in green. Although not ordinarily detectable, a small fraction of PrP is not translocated due to signal sequence inefficiency and is rapidly degraded via a transient intermediate (indicated in braces). Under conditions of ER stress (right diagrams), the availability of the putative lumenal factor is reduced due to its association with misfolded proteins (indicated in red). This causes the translocation of PrP to be reduced, leading to a greater proportion of it being degraded in the cytosol. By contrast, translocation of Opn-PrP continues with high efficiency during ER stress, leading to the accumulation of misfolded, aggregation-prone protein in the ER lumen. The left diagrams show the consequenes of partial proteasome inhibition, which may occur during aging or the course of certain neurodegenerative diseases (Gray et al., 2003; Ciechanover and Brundin, 2003). Under these conditions, PrP, due to its slightly inefficient translocation, generates cytosolic aggregates that are not formed with Opn-PrP.

Supplemental References

Anjos, S., Nguyen, A., Ounissi-Benkalha, H., Tessier, M. C., and Polychronakos, C. (2002). A common autoimmunity predisposing signal peptide variant of the cytotoxic T-lymphocyte antigen 4 results in inefficient glycosylation of the susceptibility allele. J Biol Chem 277, 46478-46486.

Ciechanover, A., and Brundin, P. (2003). The ubiquitin proteasome system in neurodegenerative diseases: sometimes the chicken, sometimes the egg. Neuron 40, 427-446.

Drisaldi, B., Stewart, R. S., Adles, C., Stewart, L. R., Quaglio, E., Biasini, E., Fioriti, L., Chiesa, R., and Harris, D. A. (2003). Mutant PrP is delayed in its exit from the endoplasmic reticulum, but neither wild-type nor mutant PrP undergoes retrotranslocation prior to proteasomal degradation. J Biol Chem 278, 21732-21743. Epub 22003 Mar 21726.

Fons, R. D., Bogert, B. A., and Hegde, R. S. (2003). Substrate-specific function of the translocon-associated protein complex during translocation across the ER membrane. J Cell Biol 160, 529-539.

Garcia, P. D., Ou, J. H., Rutter, W. J., and Walter, P. (1988). Targeting of the hepatitis B virus precore protein to the endoplasmic reticulum membrane: after signal peptide cleavage translocation can be aborted and the product released into the cytoplasm. J Cell Biol 106, 1093-1104.

Garrison, J. L., Kunkel, E. J., Hegde, R. S., and Taunton, J. (2005). A substrate-specific inhibitor of protein translocation into the endoplasmic reticulum. Nature 436, 285-289.

Gorlich, D., and Rapoport, T. A. (1993). Protein translocation into proteoliposomes reconstituted from purified components of the endoplasmic reticulum membrane. Cell 75, 615-630.

Gray, D. A., Tsirigotis, M., and Woulfe, J. (2003). Ubiquitin, proteasomes, and the aging brain. Sci Aging Knowledge Environ 2003, RE6.

Hamman, B. D., Hendershot, L. M., and Johnson, A.E. (1998) BiP maintains the permeability barrier of the ER membrane by sealing the lumenal end of the translocon pore before and early in translocation. Cell 92, 747-758.

Hegde, R. S., and Lingappa, V. R. (1996). Sequence-specific alteration of the ribosome-membrane junction exposes nascent secretory proteins to the cytosol. Cell 85, 217-228.

Hegde, R. S., Mastrianni, J. A., Scott, M. R., DeFea, K. A., Tremblay, P., Torchia, M., DeArmond, S. J., Prusiner, S. B., and Lingappa, V. R. (1998a). A transmembrane form of the prion protein in neurodegenerative disease. Science 279, 827-834.

Hegde, R. S., Voigt, S., Rapoport, T. A., and Lingappa, V. R. (1998b). TRAM regulates the exposure of nascent secretory proteins to the cytosol during translocation into the endoplasmic reticulum. Cell 92, 621-631.

Kim, S. J., and Hegde, R. S. (2002). Cotranslational partitioning of nascent prion protein into multiple populations at the translocation channel. Mol Biol Cell 13, 3775-3786.

Kim, S. J., Mitra, D., Salerno, J. R., and Hegde, R. S. (2002). Signal sequences control gating of the protein translocation channel in a substrate-specific manner. Dev Cell 2, 207-217.

Levine, C. G., Mitra, D., Sharma, A., Smith, C. L., and Hegde, R. S. (2005). The Efficiency of Protein Compartmentalization into the Secretory Pathway. Mol Biol Cell.

Lu, P. D., Jousse, C., Marciniak, S. J., Zhang, Y., Novoa, I., Scheuner, D., Kaufman, R. J., Ron, D., and Harding, H. P. (2004). Cytoprotection by pre-emptive conditional phosphorylation of translation initiation factor 2. Embo J 23, 169-179.

Menetret, J. F., Hegde, R. S., Heinrich, S. U., Chandramouli, P., Ludtke, S. J., Rapoport, T. A., and Akey, C. W. (2005). Architecture of the ribosome-channel complex derived from native membranes. J Mol Biol 348, 445-457.

Nicchitta, C. V., and Blobel, G. (1993). Lumenal proteins of the mammalian endoplasmic reticulum are required to complete protein translocation. Cell 73, 989-998.

Ooi, C. E., and Weiss, J. (1992). Bidirectional movement of a nascent polypeptide across microsomal membranes reveals requirements for vectorial translocation of proteins. Cell 71, 87-96.

Ott, C. M., and Lingappa, V. R. (2004). Signal sequences influence membrane integration of the prion protein. Biochemistry 43, 11973-11982.

Rane, N. S., Yonkovich, J. L., and Hegde, R. S. (2004). Protection from cytosolic prion protein toxicity by modulation of protein translocation. EMBO J 23, 4550-4559. Epub 2004 Nov 4554.

Rutkowski, D. T., Lingappa, V. R., and Hegde, R. S. (2001). Substrate-specific regulation of the ribosome- translocon junction by N-terminal signal sequences. Proc Natl Acad Sci U S A 98, 7823-7828.

Rutkowski, D. T., Ott, C. M., Polansky, J. R., and Lingappa, V. R. (2003). Signal sequences initiate the pathway of maturation in the endoplasmic reticulum lumen. J Biol Chem 278, 30365-30372.

Scheuner, D., Mierde, D. V., Song, B., Flamez, D., Creemers, J. W., Tsukamoto, K., Ribick, M., Schuit, F. C., and Kaufman, R. J. (2005). Control of mRNA translation preserves endoplasmic reticulum function in beta cells and maintains glucose homeostasis. Nat Med 11, 757-764.

Scheuner, D., Song, B., McEwen, E., Liu, C., Laybutt, R., Gillespie, P., Saunders, T., Bonner-Weir, S., and Kaufman, R. J. (2001). Translational control is required for the unfolded protein response and in vivo glucose homeostasis. Mol Cell 7, 1165-1176.

Sciaky, N., Presley, J., Smith, C., Zaal, K. J., Cole, N., Moreira, J. E., Terasaki, M., Siggia, E., and Lippincott-Schwartz, J. (1997). Golgi tubule traffic and the effects of brefeldin A visualized in living cells. J Cell Biol 139, 1137-1155.

Stewart, R. S., and Harris, D. A. (2001). Most pathogenic mutations do not alter the membrane topology of the prion protein. J Biol Chem 276, 2212-2220.

Tan, S., Wood, M., and Maher, P. (1998). Oxidative stress induces a form of programmed cell death with characteristics of both apoptosis and necrosis in neuronal cells. J Neurochem 71, 95-105.

Turner, G. C., and Varshavsky, A. (2000). Detecting and measuring cotranslational protein degradation in vivo. Science 289, 2117-2120.

Voigt, S., Jungnickel, B., Hartmann, E., and Rapoport, T. A. (1996). Signal sequence-dependent function of the TRAM protein during early phases of protein transport across the endoplasmic reticulum membrane. J Cell Biol 134, 25-35.